Condensed matter theory

Lecture notes and problem sets 2014/2015

Dmitri Ivanov

Contents

Recommended books

General topics:

[AM] N. W. Ashcroft and N. D. Mermin, *Solid State Physics*.

[Mar] M. P. Marder, *Condensed Matter Physics*.

Group representation theory and its application to electronic band structure:

[DV] D. Vvedensky, Group Theory, lecture notes of a course at the Imperial College London: `http://www.cmth.ph.ic.ac.uk/people/d.vvedensky/courses.html`.

[BP] F. Bassani and G. Pastori Parravicini, *Electronic states and optical transitions in solids* (Pergamon Press, Oxford, 1975)

[DDJ] M. S. Dresselhaus, G. Dresselhaus, and A. Jorio, *Group theory: Applications to the physics of condensed matter* (Springer, Berlin, 2008)

Second quantization and many-body methods:

[BR] J.-P. Blaizot et G. Ripka, *Quantum theory of finite systems* (MIT press, 1985).

[PC] Piers Coleman, *Introduction to Many-Body Physics*.

BCS theory of superconductivity

[LP] E. M. Lifshitz and L. P. Pitaevskii, *Statistical Physics, Part 2* (vol.9 of *Landau et Lifshitz*), Sections 39,40.

1 Introduction

Ref: [AM].

1.1 Electrons in metals: methods and approximations

In solid state theory, one is interested in the physics of the interacting electrons and nuclei (the latter are usually ordered in a crystal). While the microscopic nature of interactions is known, finding the resulting effective behavior is a challenging task. Generally, the Hamiltonian of the system has the form

$$H = T_e + T_N + V_{ee} + V_{eN} + V_{NN} \,. \tag{1.1.1}$$

where T_e and T_N are the kinetic energies of the electrons and nuclei, and V_{ee}, V_{eN}, V_{NN} are the interactions (of which the strongest are the electrostatic Coulomb interactions, but spin-orbit interactions may also be relevant). Solving this complicated many-body problem exactly is impossible (even numerically), and various levels of approximations are used. We can mention several commonly used levels of approximations:

- **Drude theory of conductivity.** This approximation describes electrons *classically* and neglects the role of nuclei (except for impurities). See your course of General Physics and [AM] chapter 1.
- **Free-fermion approximation (Sommerfeld theory).** Treating electrons as free *quantum* particles (fermions). The periodic potential of nuclei is still neglected. See your course of Solid State Physics and [AM] chapter 2.
- **Band theory.** Quantum particles in a periodic potential of the nuclei. See your course of Solid State Physics and [AM] chapter 8.
- **Including electron-electron interactions.** Electron-electron interaction can be included at various levels of approximation: Hartree–Fock, random-phase-approximation (RPA), Landau Fermi liquid.
- **Numerical methods.** Interactions may also be studied with numerical methods: ab initio calculations, density functional theory.
- **Including electron-phonon interactions.** In some situations, these interactions may be important. For example, they provide an important mechanism of resistivity at high temperatures. They are also responsible for attraction between electrons leading to superconductivity.

In the first lecture, we briefly review the advantages and limitations of these methods and outline the program for the course.

1.1.1 Classical Drude theory

Ref: [AM] Chapter 1.

This is the simplest model of a metal (proposed by Drude in 1900). The electrons are treated as classical particles scattering randomly at impurities. Scattering on impurities

is parametrized by the "relaxation time" τ (the time after which the electron randomly changes the direction of its motion). Then, from simple classical arguments (see your physics course) one finds the DC electrical conductivity

$$\sigma = \frac{ne^2\tau}{m}\,. \tag{1.1.2}$$

Here m is the electron mass and n is the density of electrons.

A similar calculation may be done for the thermal conductivity leading to

$$\kappa = \frac{1}{3}v^2\tau c_V\,, \tag{1.1.3}$$

where v^2 is the mean square electronic speed and c_V is the electronic specific heat. For the classical ideal gas model,

$$v^2 = \frac{3k_BT}{m}\,, \qquad c_V = \frac{3}{2}nk_B\,, \qquad \begin{array}{l}\text{* these formulas are incorrect}\\ \text{for quantum electrons (fermions)}\end{array} \tag{1.1.4}$$

leading to

$$\kappa = \frac{3nk_B^2\tau T}{2m} \qquad \begin{array}{l}\text{* the numerical coefficient is incorrect}\\ \text{for quantum electrons (fermions)}\end{array} \tag{1.1.5}$$

and further to the "Wiedemann–Franz law" (with a wrong coefficient)

$$\frac{\kappa}{\sigma} = \frac{3}{2}\left(\frac{k_B}{e}\right)^2 T\,. \qquad \begin{array}{l}\text{* the numerical coefficient is incorrect}\\ \text{for quantum electrons (fermions)}\end{array} \tag{1.1.6}$$

Experimentally, indeed, the ratio κ/σ is roughly proportional to T, but the proportionality coefficient is approximately two times larger (see Table 1.6 in [AM]). It turns out, however, that this qualitative agreement with experiment is due to a cancellation of two mistakes: both estimates in Eq. (1.1.4) are wrong, even though their product has a correct order of magnitude (see our discussion of the *quantum* theory in the next section).

Furthermore, the discrepancy with experiment is much larger if one considers the thermoelectric effect (the Seebeck effect: $\mathbf{E} = Q\nabla T$). In the Drude model, one finds for the thermoelectric coefficient

$$Q = -\frac{c_V}{3ne} = -\frac{k_B}{2e} = -0.43\cdot 10^{-4}\text{volt/K}\,, \tag{1.1.7}$$

which is two orders of magnitude larger than the experimentally observed values.

One concludes that a *quantum* theory is needed for an accurate description of electrons in metals.

1.1.2 Sommerfeld theory of metals

Ref: [AM] Chapter 2.

In this theory, we treat electrons as a gas of free fermions. The main results are:

1. Linear in T specific heat [note a huge difference from the classical result (1.1.4)].

2. The Drude expression (1.1.2) for the conductivity remains unchanged, as long as the motion of electrons is quasiclassical (i.e. the mean free path is much longer than the wave length), which is typically satisfied, and provided we can describe collisions by a single (independent of energy and momentum) relaxation time τ (which is a more subtle condition).

3. The expression (1.1.3) for the thermal conductivity remains valid, but the mean square velocity and the specific heat are given now by

$$v^2 = v_F^2 = \frac{2\varepsilon_F}{m}\,, \qquad c_V = \frac{\pi^2 n k_B^2 T}{2\varepsilon_F}\,. \tag{1.1.8}$$

   This results in a more accurate coefficient in the Wiedemann–Franz law:

$$\frac{\kappa}{\sigma} = \frac{\pi^2}{3}\left(\frac{k_B}{e}\right)^2 T\,. \tag{1.1.9}$$

4. Thermopower: If we use the specific heat from Eq. (1.1.8) for calculating the thermopower, we get a reasonable estimate

$$Q = -\frac{\pi^2}{6}\,\frac{k_B}{e}\left(\frac{k_B T}{\varepsilon_F}\right)\,, \tag{1.1.10}$$

   which is smaller than in the classical Drude theory by a factor of about $(k_B T/\varepsilon_F)$ (two orders of magnitude at room temperature).

5. Spin susceptibility: The spin susceptibility is temperature independent at low temperatures (see, e.g. the condensed-matter-physics course).

Overall, this approximation gives a good description of the quantum behavior of conduction electrons, but becomes inaccurate for properties depending on the geometry of the Fermi surface or on the interactions.

1.1.3 Band theory

As you have learned in previous physics courses, nuclei in solids form regular periodic patterns: crystals. You have discussed the symmetry properties and classification of crystal lattices in the course of condensed matter physics.

The crystal lattice of nuclei produces a periodic potential for electrons. Single-particle quantum states in such a potential are not localized, but are periodic in space: Bloch waves forming bands.

This theory can explain:

1. Why some materials are metals and some insulators.

2. For metals, properties depending on the shape of the Fermi surface (de Haas–van Alphen effect, sign of the Hall coefficient, etc.)

In our lectures, we will discuss the role of the crystal symmetry in the band structure.

1.1.4 Including interactions: Hartree–Fock, Landau Fermi liquid, Density functional theory, etc.

All the methods discussed above treat electrons as non-interacting. For some physical effects, interactions *are* important.

In some situations, interactions may be taken into account analytically by renormalizing in some way the non-interacting model (Hartree–Fock, random-phase approximation, Landau Fermi Liquid theory). For more accurate estimates of the role of interactions on the electronic structure, one uses more sophisticated numerical methods (e.g., density functional theory).

In other situations, interactions lead to qualitatively new physics. One example, which we will discuss in our course: superconductivity (BCS theory). The BCS theory is a good textbook example, because a simple analytic theory exists. There are many other physical examples, where such a simple theory has not been yet developed (if it exists at all): high-temperature superconductivity, fractional quantum Hall effect, etc.

1.1.5 Estimating the importance of interactions

Consider a free electron gas of density n. A typical distance between electrons r_s may be defined as the radius of the sphere whose volume equals the volume per one electron:

$$\frac{V}{N} = \frac{1}{n} = \frac{4\pi r_s^3}{3}, \qquad r_s = \left(\frac{3}{4\pi n}\right)^{1/3} \tag{1.1.11}$$

It is also convenient to measure r_s in the units of the Bohr radius

$$a_0 = \frac{\hbar^2}{me^2} = 0.529\text{Å} \tag{1.1.12}$$

The typical kinetic energy is of the order of the Fermi energy (below I do not keep track of numerical coefficients):

$$E_F \sim \frac{\hbar^2 k^2}{m} \sim \frac{\hbar^2}{r_s^2 m} \tag{1.1.13}$$

while the typical interaction energy is

$$E_C \sim \frac{e^2}{r_s} \tag{1.1.14}$$

The importance of interaction is determined by the ratio

$$\frac{E_C}{E_F} \sim \frac{me^2 r_s}{\hbar^2} = \frac{r_s}{a_0} \tag{1.1.15}$$

— i.e., the interaction is more important at *low* densities!

It was predicted theoretically that at very low densities the interactions become so strong that fermions crystallize at zero temperature (E. Wigner, 1934). Numerical studies suggest that such a crystallization occurs at $r_s/a_0 \sim 106$ in 3D and $r_s/a_0 \sim 31$ in 2D. For typical metals, r_s/a_0 is of the order 2–5.

1.1.6 Plan of the course (approximate)

- **Lecture 1.** Specific heat and transport properties in the model of noninteracting fermions.
- **Lectures 2-3.** Electronic energy bands in crystals. Role of crystal symmetries. (Introduction to the theory of group representations.)
- **Lectures 4-5-6-7-8.** Interactions between electrons. Perturbative approach, Hartree–Fock, screening of interactions. (Second quantization and introduction to diagrammatic methods.)
- **Lecture 9-10.** Phonons, electron-phonon interaction.
- **Lecture 11-12.** BCS theory of superconductivity.

1.2 Specific heat and transport properties in the model of noninteracting fermions.

In this section, we derive the specific heat (1.1.8), the electrical conductivity (1.1.2), and the thermal conductivity (1.1.3) in the model of noninteracting fermions. We will present the calculations in a form suitable for both the Sommerfeld theory (spherical Fermi surface) and the band theory (for an arbitrary shape of the Fermi surface).

1.2.1 Specific heat

Ref: [AM] Chapter 2.

Specific heat is an *equilibrium* characteristic of a statistical system:

$$c_V = \frac{\partial \mathcal{E}}{\partial T}\,, \tag{1.2.1}$$

where $\mathcal{E}$ is the energy at thermal equilibrium at a given temperature T. At equilibrium, every single-particle level (at a given energy E_i) can be treated independently: it is either empty or occupied, with the probabilities given by the Fermi–Dirac distribution:

$$p_0 = \frac{1}{1+\exp[-(E_i-E_F)/T]}\,, \qquad p_1 = n_F(E_i) = \frac{\exp[-(E_i-E_F)/T]}{1+\exp[-(E_i-E_F)/T]}\,. \tag{1.2.2}$$

Then the total energy can be calculated as

$$\mathcal{E}(T) = \sum_i E_i\, n_F(E_i)\,. \tag{1.2.3}$$

It only depends on the energy levels, but not on the properties of the eigenstates. Then it is convenient to introduce the *density of states* $\nu(E)$: the number of energy levels per unit of energy per unit of volume. Then the sum can be re-expressed as an integral

$$\mathcal{E}(T) = \int E\, n_F(E)\, \nu(E)\, dE \tag{1.2.4}$$

(energy per unit volume), and the specific heat then equals

$$c_V = \int E \frac{\partial}{\partial T} n_F(E)\, \nu(E)\, dE \tag{1.2.5}$$

Under the condition that the temperature is sufficiently low so that we can neglect the energy dependence of $\nu(E)$ in the corresponding energy window around the Fermi level, we can approximate

$$c_V = \nu(E_F) \int E \frac{\partial}{\partial T} n_F(E)\, dE\,. \tag{1.2.6}$$

After calculating the integral, one arrives at a general expression linear in T and in $\nu(E_F)$ (see Problem 1.1), which, in the case of the free fermion gas, further reduces to Eq. (1.1.8).

Note that this result for the specific heat (linear in T) is only relevant at very low temperatures, where c_V is dominated by electrons. At higher temperatures, the phonon contribution (proportional to T^3) comes in.

1.2.2 Electrical and thermal conductivities

Ref: [AM] Chapter 13.

Calculating electrical and thermal conductivities is a more complicated problem, even in a non-interacting model, since it requires taking into account a non-equilibrium distribution of electrons. We make two assumptions for our calculation:

- quasiclassical regime (mean free path of electrons is much larger than their wave length)
- relaxation-time approximation: relaxation processes lead to relaxation to a thermal equilibrium characterized by a single time scale τ (independent of the momentum and energy of the electron).

Under the quasiclassical assumption, we can describe the state of the electrons by the occupation number $n(k, r)$ as a function of *both* momentum and coordinate. Under the relaxation-time approximation, we can write the kinetic equation

$$\frac{\partial}{\partial t} n = -\frac{n - n_F}{\tau} - \mathbf{v} \frac{\partial}{\partial \mathbf{r}} n - e\mathbf{E} \frac{\partial}{\partial \mathbf{k}} n\,. \tag{1.2.7}$$

Here the first term describes the equilibration towards the Fermi–Dirac distribution (at a given temperature) n_F, the second term describes the ballistic transfer of the distribution function with the velocity $\mathbf{v}(k) = \partial E(k)/\partial k$ and the last term includes the acceleration of electrons by the electric field $\mathbf{E}$.

We can compute the response of the electric current $\mathbf{j}$ to the electric field $\mathbf{E}$ by assuming a homogeneous non-equilibrium distribution $n = n_F + \delta n$. To the leading order, we can solve for δn:

$$\delta n = -\tau e \mathbf{E} \mathbf{v} \frac{\partial}{\partial E} n_F\,, \tag{1.2.8}$$

while the current is given by

$$\mathbf{j} = e \int \frac{d^3k}{(2\pi)^3}\, \mathbf{v}\, \delta n\,. \tag{1.2.9}$$

This immediately leads to the expression for the tensor of electrical conductivity (defined as $\mathbf{j}_\alpha = \sigma_{\alpha\beta}\mathbf{E}_\beta$):

$$\sigma_{\alpha\beta} = -e^2\tau \int \frac{d^3k}{(2\pi)^3}\, v_\alpha v_\beta \frac{\partial}{\partial E} n_F \,. \tag{1.2.10}$$

Note that this expression, at low temperature, only weakly depends on temperature and is determined only by the energy dispersion in the vicinity of the Fermi surface. For the quadratic spectrum, it reduces to the Drude expression (1.1.2) (see Problem 1.2).

In a similar way, one can calculate the thermal conductivity. The delicate point here is that the thermal conductivity is defined as the energy flow under the condition of the *zero electric current*. This condition can be taken into account, to the leading order, if we compute the energy current as

$$\mathbf{j}_E = \int \frac{d^3k}{(2\pi)^3}(E - E_F)\mathbf{v}\delta n \,. \tag{1.2.11}$$

The out-of-equilibrium part of the distribution function δn can be computed from Eq. (1.2.7) with $\partial n/\partial t = 0$, $\mathbf{E} = 0$, and $\partial n/\partial \mathbf{r} = (\nabla T)\partial n_F/\partial T$. As a result, we find for the tensor of thermal conductivity (defined as $(\mathbf{j}_E)_\alpha = -\kappa_{\alpha\beta}(\nabla T)_\beta$):

$$\kappa_{\alpha\beta} = \tau \int \frac{d^3k}{(2\pi)^3} v_\alpha v_\beta (E - E_F)\frac{\partial}{\partial T} n_F \,. \tag{1.2.12}$$

This expression has a structure similar to Eq. (1.2.10). At low temperature, both expressions are proportional to the integral over the Fermi surface:

$$\int dS \frac{v_\alpha v_\beta}{v} \tag{1.2.13}$$

(see Problem 1.2), and their ratio obeys the Wiedemann–Franz law (1.1.9).

In reality, the Wiedemann–Franz law is not always obeyed. The main limitation comes from the relaxation-time approximation. The validity of this approximation depends on the mechanism of relaxation and on the temperature (which determines the typical energy range of electrons). For elastic scattering on impurities, in isotropic systems, the relaxation-time approximation can be rigorously derived (we will not do it in our lectures, see [AM] Chapter 16). For electron-electron scattering, it is applicable only qualitatively. For electron-phonon scattering, it is invalid at low temperatures, but works at high temperatures. As a result, the Wiedemann–Franz law is often applicable at high temperatures (room temperature and above) and at very low temperatures, but does not apply in the intermediate temperature range. For illustration, see Table 1.6 in [AM]. For more details on the applicability of the relaxation-time approximation, see, e.g., the book by A. A. Abrikosov "Fundamentals of the Theory of Metals".

2 Electronic band structure and lattice symmetries

In this section, we discuss how crystal symmetries can help in describing the electronic band structure (in particular, the level degeneracies at points of special symmetry in the Brillouin zone). In fact, the band structure itself (Bloch waves) may be viewed as a consequence of the translational symmetry of the crystal lattice.

2.1 Symmetries in quantum mechanics. Introductory remarks

Symmetries play an important role in quantum mechanics. If a quantum problem has symmetries, then

- symmetries simplify the problem by providing good "quantum numbers"
- symmetries may be responsible for levels degeneracies

Namely, quantum levels may be classified according to the irreducible representations of the symmetry group. Then the Hamiltonian may be projected onto the states belonging to a specific type of irreducible representations, which reduces the dimension of the Hilbert space and thus simplifies the problem. If this irreducible representation is more than one-dimensional, then the corresponding levels are accordingly degenerate.

An example of such a reduction is known from a course of quantum mechanics: for a particle in a centrally symmetric potential, the states may be classified according to their angular momentum. In our course we will consider another example: how the *symmetries of the crystal lattice* may be used to classify electronic states.

The crystal symmetries involve two types of operations:

- Translations. These symmetries are responsible for the band structure: the states are classified according to their wave vectors ("Bloch theorem").
- Rotations and reflections. These symmetries are responsible for additional degeneracies occurring in the band structure.

Before discussing these symmetries in more detail, we briefly review the theory of group representations.

2.2 Groups and their representations: A crash course

Ref: [DV].

Please check the properties mentioned below against an example of your favorite group!

2.2.1 Definition of a group

A *group* is a set of elements with a multiplication operation. The multiplication must obey the following properties:

- $(ab)c = a(bc)$ — associativity
- $1 \cdot a = a \cdot 1 = a$ — the existence of unity (can you prove its uniqueness?)
- $aa^{-1} = a^{-1}a = 1$ — the existence of an inverse (one can further prove its uniqueness)

Groups often appear as symmetries of a geometric or physical object (atom, molecule, crystal). Think of examples of discrete and continuous groups.

2.2.2 Subgroups and direct product of groups

A *subgroup* is a group within a group (with the same multiplication operation). Think of interesting examples.

A *direct product* of two groups G and H is a set of pairs (g, h) with $g \in G$, $h \in H$, and a natural definition of multiplication: $(g_1, h_1) \cdot (g_2, h_2) = (g_1 g_2, h_1 h_2)$. Think of physical examples of this construction.

2.2.3 Abelian and nonabelian groups. Classes of conjugate elements

A group is said to be *abelian* if all its elements commute, $ab = ba$, and *nonabelian* otherwise. Example: rotations in 2D form an abelian group, rotations in 3D are nonabelian.

If we pick an element u in a group G, it defines a "similarity" (or *conjugation*) transformation $g \mapsto ugu^{-1}$ (for all elements $g \in G$). This similarity preserves the group multiplication: $(ug_1u^{-1})(ug_2u^{-1}) = u(g_1g_2)u^{-1}$. In other words, it is a symmetry of the group.

Abelian groups do not have nontrivial conjugations.

All elements related by conjugations form a *class of conjugate elements* (they are "similar" to each other). Example: in 3D, all rotation by a given angle (independently of the axis of rotation) are conjugate to each other.

2.2.4 Representations of groups

A (linear) *representation* of a group G is a set of $n \times n$ matrices which have the same multiplication table (with respect to the matrix product) as the group elements: to each group element g, there corresponds an *invertible* matrix $D(g)$ such that

$$D(g_1)D(g_2) = D(g_1 g_2)\,. \tag{2.2.1}$$

The *dimension* of the representation is the size n of those matrices.

Example 1. If the group corresponds to spatial rotations of some object, than these spatial symmetries (written as coordinate transformations in space) realize its representation. The dimension of this representation equals the dimension of the physical space.

Example 2. For any group, there exists a one-dimensional trivial (identity) representation: matrices 1×1 (just numbers) with $D(g) \equiv 1$.

Example 3. For any group, there exists a so called *regular representation*. It is constructed in the following way. Consider group elements g as a basis of (quantum) states $|g\rangle$ and consider all possible superpositions

$$\psi = \sum_{g \in G} c_g \,|g\rangle\ . \tag{2.2.2}$$

Now if we define the action of a group element g_1 on the basis states by permuting them according to the group multiplication,

$$D(g_1)\,|g_2\rangle = |g_1 g_2\rangle\ , \tag{2.2.3}$$

then this action can be extended to a linear transformation on all the states ψ:

$$D(g) \sum_{g' \in G} c_{g'}\,|g'\rangle = \sum_{g' \in G} c_{g'}\,|gg'\rangle \tag{2.2.4}$$

and written as a matrix of the size equal to the number of elements in the group G. In the basis of the states $|g\rangle$, these matrices only contain zeros and ones. One can easily see that they form a representation of G.

This regular representation is useful in the representation theory, since it contains all the irreducible representations of the group (see below).

2.2.5 Reducible and irreducible representations

If some similarity transformation (change of basis)

$$D'(g) = UD(g)U^{-1} \tag{2.2.5}$$

with some matrix U (the same for all the elements g) brings a representation into a block-diagonal form

$$D'(g) = \begin{pmatrix} D'_1(g) & 0 \\ 0 & D'_2(g) \end{pmatrix} \tag{2.2.6}$$

(with some square matrices $D'_1(g)$ and $D'_2(g)$), then this representation is said to be *reducible* (and the representation $D(g)$ is decomposed into the *sum* of $D'_1(g)$ and $D'_2(g)$). Otherwise, it is called *irreducible*.

Note: if a representation is reducible, then there is a smaller subspace invariant with respect to all the elements of the group.

The reverse is true, if the representation is *unitary* (all $D(g)$ are unitary matrices).

- In general, any representation of a *finite* or, more generally, *compact* group can be brought to a unitary form by a suitable change of basis (2.2.5). For a counterexample (a representation of a non-compact group which cannot be brought to a unitary form), see the discussion of the translational symmetry of the lattice in the next lecture.

- In application to quantum mechanics, we always assume that our representations are unitary, since they correspond to physical symmetries of the Hilbert space of quantum states and hence are represented by unitary matrices.

Example. Consider the group of permutations of the three coordinate axes in the 3D space (6 permutations in total, this group is usually denoted S_3). Those permutations of the axes realize a three-dimensional representation of the group. The diagonal $x = y = z$ is invariant with respect to all those permutations. Therefore we immediately deduce that this representation is reducible.

2.2.6 Characters and character tables. Orthogonality relations

Our goal in this lecture is to learn how to

- classify all irreducible representations of a given group;

- for a given representation (physical symmetry acting in a physical Hilbert space of quantum states), decompose it into a sum of irreducible representations.

This can be done with the help of characters.

A *character* of a representation $D(g)$ is a numerical function on the group elements defined as

$$\chi_D(g) = \operatorname{tr} D(g) \tag{2.2.7}$$

(trace of the matrix). It can be thought of as a fingerprint of a representation.

Some obvious properties of the character:

- $\chi_D(g)$ is basis independent;
- $\chi_D(g)$ is the same for all elements g in one class of conjugate elements. So the character is in fact a function on classes of conjugate elements;
- for any representation D, $\chi_D(1)$ gives the dimension of the representation (since 1 is always represented by the unit matrix);
- The character of a sum of representations (2.2.6) equals the sum of their characters.

For a finite group, the number of irreducible representations is also finite, and it is convenient to list the characters of all its irreducible representations in a table: the rows of the table correspond to the representations, the columns — to the classes of conjugate elements.

Example. The group S_3 of all the permutations of three elements. It has 6 group elements, which form three conjugate classes:

- identity element, 1, is always alone in its class
- three pairwise permutations, (12), (23) and (13). We denote this class $3_{(12)}$
- two cyclic permutations of the three elements, (123) and (132). We denote this class $2_{(123)}$

The representation table for S_3 looks as follows:

	1	$3_{(12)}$	$2_{(123)}$
Γ_1	1	1	1
Γ_2	1	-1	1
Γ_3	2	0	-1

For any group, its table of irreducible representations obeys the orthogonality relations (we don't prove them here, please refer to [DV] for proofs):

- **Orthogonality of rows:**

$$\sum_\alpha n_\alpha \chi_k(\alpha)\chi_{k'}(\alpha)^* = |G|\delta_{kk'}\,, \tag{2.2.8}$$

where the sum is taken over classes of conjugate elements, n_α is the number of elements in each class, and $|G|$ is the total number of elements in the group. k and k' denote two (different or coinciding) irreducible representations. The star denotes complex conjugation (characters are sometimes complex!).

- **Orthogonality of columns:**

$$\sum_k \chi_k(\alpha)\chi_k(\alpha')^* = \frac{|G|}{n_\alpha}\delta_{\alpha\alpha'}\,, \tag{2.2.9}$$

  where the sum is now over irreducible representations.

Several useful properties follow from these general orthogonality relations (or can be deduced independently):

- The number of irreducible representations of the group equals the number of conjugacy classes of that group;
- The sum of squares of the dimensions of the irreducible representations equals the number of elements in the group:

$$\sum_k \dim(k)^2 = |G| \tag{2.2.10}$$

  Note that these two properties are usually sufficient to determine the dimensions of the irreducible representations for sufficiently small finite groups.

- Abelian (commutative) groups have only one-dimensional irreducible representations. Nonabelian (noncommutative) groups have at least one non-one-dimensional irreducible representation.

For sufficiently small finite groups, the character tables may be constructed "by hand": usually, one knows a priori some of the representations (e.g., the identity representation and other one-dimensional representations), and, together with the orthogonality relations, it is sufficient to complete the table. Formal algorithms also exist, but they are more suitable for computer programs and we will not study them.

Furthermore, the orthogonality relations help in decomposing a given representation into a sum of irreducible representations. This can be done by *projecting* onto each irreducible representation using (2.2.8):

$$N_k = \frac{1}{|G|}\sum_\alpha n_\alpha \chi(\alpha)\chi_k(\alpha)^*\,. \tag{2.2.11}$$

In particular, if we apply this formula to the *regular representation* (whose character is $\chi(1) = |G|$ and $\chi(\alpha) = 0$ for all other conjugacy classes), we find that the fundamental representation contains all the irreducible representations with multiplicities equal to their dimensions [cf. Eq. (2.2.10)].

2.2.7 Irreducible representations in quantum mechanics

Suppose now that G is the group of symmetries of a quantum Hamiltonian H. Then it is represented by linear (unitary) operators in the Hilbert space of quantum states.

Usually, this representation is reducible. The symmetry of the Hamiltonian implies $D(g)HD(g)^{-1} = H$ for all group elements g.[1]

Suppose, Ψ is an eigenstate of H at energy E. Then, for any group element g, its action on Ψ produces again an eigenstate at the same energy E. Formally, we may write this as

$$HD(g)\Psi = D(g)H\Psi = D(g)E\Psi = ED(g)\Psi\,. \tag{2.2.12}$$

If we diagonalize the Hamiltonian, then the eigenvectors corresponding to the same energy transform into each other by the group G and therefore form a representation of G.

Thus the diagonalization of the Hamiltonian simultaneously decomposes the representation of G in the full Hilbert space into a sum of smaller representation. If those smaller representations are reducible, we may decompose them further, until we reach a decomposition into irreducible representations. Each of the irreducible representations is an eigenspace of the Hamiltonian corresponding to some energy E.

In the most general situation, all those energies E are different, and we find that the degeneracies of levels are given by the dimensions of the irreducible representations. Sometimes, some of those energies may coincide, and then the degeneracy is given by the sum of the dimensions of several irreducible representations. Usually, this coincidence happens either as a result of a fine-tuning of some parameters (*accidental degeneracy*) or as a consequence of a larger symmetry not taken into account.

We can also reverse this procedure and first decompose the full representation of G into a sum of irreducible representations, and then it will be sufficient to diagonalize the Hamiltonian separately within each class of irreducible representations. This classification into irreducible representations provides a good set of "quantum numbers" and considerably simplifies the problem (by reducing the dimension of the Hamiltonian).

Example: For a quantum particle in a symmetric potential $U(x) = U(-x)$, we may require that the eigenstates are either even or odd in x: $\Psi(x) = \pm\Psi(-x)$. Those even (odd) wave functions belong to the even (odd) representation of the reflection symmetry group (transforming $x \mapsto -x$).

2.2.8 Concluding remarks

For understanding general properties of groups and their representations, it is always helpful to keep in mind some simple examples (cyclic groups, 3D rotations, etc.).

We have discussed mainly representations of *finite* groups: in this case, there is only a finite number of irreducible representations, and the character table is finite. However, many of the properties of representations of infinite groups (e.g., orthogonality relations) are very similar to the finite case, with the only difference that the number of irreducible representations becomes infinite, and the finite sums get replaced either by infinite sums or by integrals.

[1] Rigorously speaking, since quantum states are defined up to a phase factor, the group G is also represented up to arbitrary phase factors in Eq. (2.2.1). In this way, the notion of a linear representation is generalized to a *projective representation* (in the context of electronic structure, also sometimes called a *representation of the double group*). The examples of nontrivial projective representations are 3D rotations of a half-integer spin and translations of a charged particle in a magnetic field. In our lecture, we will discuss the band structure in the absence of magnetic field and neglecting the spin-orbit interaction. Under these assumptions, the geometric symmetries of the crystal lattice form a linear representation without phase factors. See however the discussion of *non-symmorphic* crystallographic groups in the next section.

2.2.9 Product of representations

Besides the *sums* of representations, one can also define their *products*. Consider two groups G and H and their direct product $G \times H$. If we have two representations D_1 and D_2 of G and H respectively, we may define their product as

$$D(g \cdot h) = D_1(g) \otimes D_2(h)\,, \tag{2.2.13}$$

where $\otimes$ is the tensor product of matrices: $(A \otimes B)_{ij,kl} = A_{ik}B_{jl}$. The dimension of such a representation equals the *product* of the dimensions of D_1 and D_2, and its character is given by the *product* of the two characters.

Note that if both D_1 and D_2 are irreducible, then their product is also irreducible (as a representation of $G \times H$). In other words, if a group is a direct product of two groups, then its table of irreducible representations can be obtained as the product of the tables of irreducible representations of its factors.

One can also encounter a situation, where the two groups G and H are equal, and their product is also viewed as a representation of the same group:

$$D(g) = D_1(g) \otimes D_2(g)\,. \tag{2.2.14}$$

In this case, the product of two irreducible representations is not generally irreducible. For example, the product of two spin-1/2 representations of the rotation group is decomposed into a singlet and a triplet (which can be symbolically written as $2 \otimes 2 = 1 \oplus 3$, if we mean by 1, 2, and 3 irreducible representations of SU(2) with the corresponding dimensions).

2.3 Band structure and lattice symmetries: example of diamond

Refs: [BP], [DDJ].

We now apply the general formalism developed in the last lecture to the example of the crystal structure of *diamond*. The first part of the discussion (about the Bloch waves) is general for any crystal structure, the rest is specific for the space group of diamond. Note that there is an additional complication for the diamond space group, since it is *non-symmorphic* (see definition below): we will remark this complication, but will not discuss it in detail. We will also not discuss the possibility of spin-orbit interactions. Please refer to literature for those details.

2.3.1 Crystal symmetries

The full symmetry of the crystal structure is usually called *space group* or *crystallographic group*. It includes *translations* (in three noncollinear directions) as a subgroup. We may further define the *point group* as a factor of the space group modulo translations. The point group is a finite group of isometries preserving one fixed point. It may contain both *proper* (preserving the orientation) and *improper* (reversing the orientation) rotations.

Sometimes, the point group is a subgroup of the space group: in this case the space group is called *symmorphic*. Otherwise (if it is not possible to realize the point group as symmetries of the crystal with one common fixed point) it is called *non-symmorphic*.

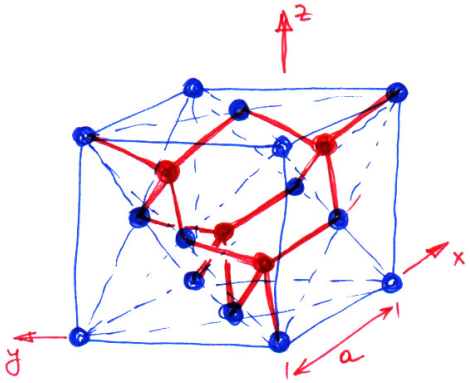

Figure 1: Diamond lattice.

2.3.2 Translational symmetries and Bloch waves

Consider first the classification of states with respect to translations. Pick the three *generating* translation vectors $\mathbf{e}_1$, $\mathbf{e}_2$, $\mathbf{e}_3$. These translations commute, so the full translational part of the crystal symmetries is a direct product of the three one-dimensional translation groups. So it is sufficient to consider each of them separately, and then take the product of the three representations.

The group of one-dimensional lattice translations is abelian and is generated by an elementary translation T. The decomposition into irreducible representations is obtained by diagonalizing the matrix T. Each eigenstate of T (called a *Bloch wave*), is multiplied by a phase factor under such an elementary translation:

$$T\Psi = e^{i\phi}\Psi\,. \tag{2.3.1}$$

Note that the we only consider the case of phase factors and disregard the possibility of eigenstates $T\Psi = c\Psi$ with $|c| \neq 1$: such eigenstates would diverge at one of the two infinities and therefore do not belong to the space of physical states. In other words, only *unitary* representations appear in physical states.

After we combine the translations along the three directions, we find for the full translation group the set of irreducible one-dimensional representations:

$$T_{n_1\mathbf{e}_1+n_2\mathbf{e}_2+n_3\mathbf{e}_3} = e^{i(n_1\phi_1+n_2\phi_2+n_3\phi_3)}\Psi\,. \tag{2.3.2}$$

The three phases ϕ_1, ϕ_2, and ϕ_3 parametrize the representation and define a point in the Brillouin zone. In other words, the Brillouin zone is the set of all irreducible representations of the translations of the crystal lattice.

If translations exhaust the symmetries of the lattice, this would be the end of the story. If, on the other hand, the point group is nontrivial, it mixes some of the points in the Brillouin zone and introduces degeneracies. Below we illustrate how it works in the example of the crystal lattice of diamond.

2.3.3 Diamond crystal lattice

The diamond crystal lattice (see Fig. 1) may be described in terms of positions of the carbon atoms. It contains two superimposed FCC (face-centered cubic) sublattices. The

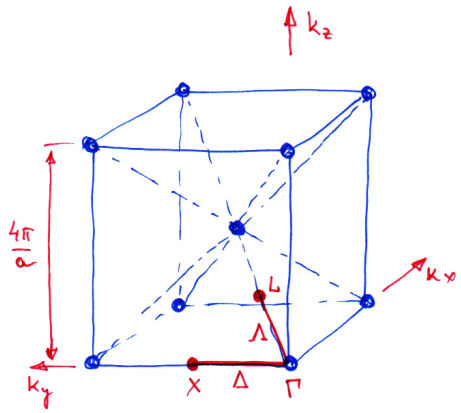

Figure 2: Dual lattice of k points and some points and lines of special symmetry.

positions of the points are:

$$\frac{a}{2}(n_1, n_2, n_3) \quad \text{and} \quad \frac{a}{2}\left(n_1 + \frac{1}{2}, n_2 + \frac{1}{2}, n_3 + \frac{1}{2}\right) \quad \text{with } (n_1 + n_2 + n_3) \text{ even.} \tag{2.3.3}$$

The lattice constant $a = 3.57$ Å (at room temperature) is the length of the side of the cube in the FCC pattern.

The elementary lattice translations are

$$\mathbf{e}_1 = \frac{a}{2}(0, 1, 1)\,, \quad \mathbf{e}_2 = \frac{a}{2}(1, 0, 1)\,, \quad \mathbf{e}_3 = \frac{a}{2}(1, 1, 0)\,. \tag{2.3.4}$$

The unit cell contains two atoms.

2.3.4 Diamond Brillouin zone

The dual lattice of k points is defined as lattice of k vectors which give trivial (multiple of 2π) phases under all translations of the lattice. From (2.3.4), we find the general formula for the lattice of k points:

$$\mathbf{k} = \frac{2\pi}{a}(-m_1 + m_2 + m_3, m_1 - m_2 + m_3, m_1 + m_2 - m_3)\,, \tag{2.3.5}$$

where m_1, m_2, and m_3 run over all integer numbers. This defines the BCC (body-centered cubic) lattice (Fig. 2).

One usually chooses the Brillouin zone (BZ) to be the set of k points that are closer to $k = 0$ than to any other k point of the lattice. This construction gives in our case the Brillouin zone in the shape of a truncated octahedron. We distinguish the points of special symmetry Γ (at $k = 0$), X [the center of a square face of the BZ, e.g., $k = (2, 0, 0)\pi/a$], and L [the center of a hexagonal face of the BZ, e.g., $k = (1, 1, 1)\pi/a$]. We also consider two lines of special symmetry: Δ (connecting Γ and X) and Λ (connecting Γ and L).

Our goal will be to find the level degeneracies at these points and on these lines.

2.3.5 Point group of the diamond lattice

If we look at the lattice of diamond (2.3.3), we find that the point group is the symmetry group of a cube (including both proper and improper rotations), but the full space group is *non-symmorphic*.

The total number of group elements of this symmetry group (denote it by O_h) is 48.

The simplest improper rotation is the inversion (the simultaneous change of sign of all the coordinates). Let us denote this transformation by I. It commutes with all the rotations, and therefore the full point group O_h can be decomposed into a *direct product* of the group of proper rotations (denoted by O, contains 24 elements) and the "inversion" group $\{0, I\}$. The latter has two irreducible representations (both are one-dimensional): the trivial one and the "parity" one. Therefore for constructing the irreducible representations of O_h, it will be sufficient to construct the representations of O and then multiply them by one of the two representations of $\{0, I\}$.

2.3.6 Representations of O and O_h

To construct the table of characters for O, start with counting the classes of conjugate elements:

1 (1 element): unity;

6_{90° (6 elements): rotations by 90 degrees;

3_{180° (3 elements): rotations by 180 degrees about a face of the cube;

6_{180° (6 elements): rotations by 180 degrees about an edge center;

8_{120° (8 elements): rotations by 120 degrees about a cube diagonal.

Total 5 classes. Therefore there will be 5 irreducible representations in the character table.

The *trivial* representation is always there. We can also guess another one-dimensional representation (denote it by P): if we color the vertices of the cube in black and white in a checkerboard pattern, then the transformations can be classified into odd and even by whether they change the color of vertices. Finally, we also know a three-dimensional representation (by considering a cube in a 3D space), which is also obviously irreducible (can you explain why?). This three-dimensional representation may, in turn, be multiplied by P to produce yet another 3D representation. So we know already 4 out of 5 irreducible representations. The last one (or rather, its character) can be found from the orthogonality relations. As a result, we find the character table of O:

	1	6_{90°	3_{180°	6_{180°	8_{120°
1	1	1	1	1	1
P	1	-1	1	-1	1
2	2	0	2	0	-1
3	3	1	-1	-1	0
$3P$	3	-1	-1	1	0

Multiplying it by the character table of $\{0, I\}$,

	1	I
1	1	1
P_I	1	-1

we can write the character table of O_h (here we use the traditional crystallographic notation for the representations):

	1	6_{90°	3_{180°	6_{180°	8_{120°	I	$I6_{90^\circ}$	$I3_{180^\circ}$	$I6_{180^\circ}$	$I8_{120^\circ}$
Γ_1	1	1	1	1	1	1	1	1	1	1
Γ_2	1	−1	1	−1	1	1	−1	1	−1	1
Γ_{12}	2	0	2	0	−1	2	0	2	0	−1
Γ'_{15}	3	1	−1	−1	0	3	1	−1	−1	0
Γ'_{25}	3	−1	−1	1	0	3	−1	−1	1	0
Γ'_1	1	1	1	1	1	−1	−1	−1	−1	−1
Γ'_2	1	−1	1	−1	1	−1	1	−1	1	−1
Γ'_{12}	2	0	2	0	−1	−2	0	−2	0	1
Γ_{15}	3	1	−1	−1	0	−3	−1	1	1	0
Γ_{25}	3	−1	−1	1	0	−3	1	1	−1	0

2.3.7 Projective representations and non-symmorphic space groups

So far, we were assuming that we indeed had a linear representation of the symmetry group in the space of electron states. In fact, quantum states are defined up to a phase factor, and the group may also be represented only up to phase factors:

$$D(g_1)D(g_2) = e^{i\phi(g_1,g_2)}D(g_1g_2)\,. \tag{2.3.6}$$

In some situations, the phase factors $\phi(g_1, g_2)$ may be compensated by redefining $D(g)$:

$$D(g) \mapsto e^{i\alpha(g)}D(g)\,, \tag{2.3.7}$$

and then the problem reduces to the conventional representation theory. In other situations, the phase factors $\phi(g_1, g_2)$ cannot be compensated, and we obtain a different type of representation, not included in the conventional character table.

The more general definition (2.3.6) of a representation is called a *projective representation*. The theory of projective representations may be reduced to the conventional theory of linear representations by extending the group (writing the phase factors as separate group elements commuting with the rest of the group) and then studying the conventional linear representations of the extended group (sometimes called the *double group* in the crystallographic context).

Examples of nontrivial projective representations include 3D rotations of a half-integer spin and translations of a charged particle in a magnetic field. In our example, we neglect the spin-orbit interaction, so no phase factors appear due to spin. However, one still needs to consider projective representations in order to classify the energy levels at some points at the boundary of the Brillouin zone in the case of a *non-symmorphic* space group. In our lecture, we will skip this part of the calculation.

2.3.8 Free-electron band structure

As a very crude approximation of the low-lying states, we may consider the band structure for a free electron by folding the parabolic spectrum centered at the lattice of k vectors (2.3.5) onto the BZ. This way we get the structure shown in Fig. 3. Note the very high degeneracies of levels. These degeneracies are reduced in a lattice potential down to the dimensions of the corresponding irreducible representations.

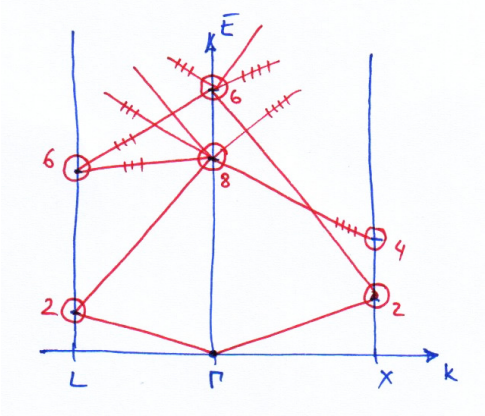

Figure 3: Sketch of the free-electron band structure of the diamond. Level degeneracies are marked.

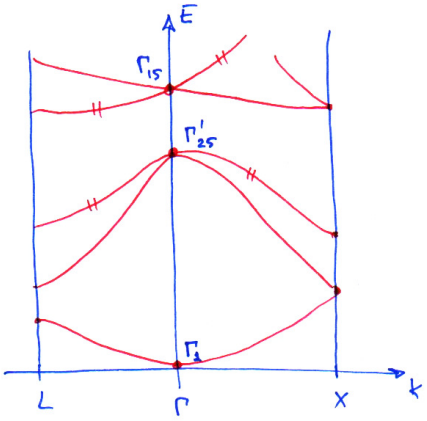

Figure 4: Sketch of the actual band structure of diamond, as calculated numerically in Bassani and Yoshimine, Phys. Rev. **130**, 20 (1963).

2.3.9 Numerically calculated band structure

The band structure calculated with a numerical method (orthogonalized plane wave) is schematically shown in Fig. 4. The degeneracies can be understood in terms of irreducible representations as discussed below.

2.3.10 Classification of states at the point Γ

The symmetry operations of the space group may be written as

$$g : x \mapsto Rx + L\,, \tag{2.3.8}$$

where R is an element of the point group (with respect to some center) and L is a translation. At the point Γ, translations do not produce extra phase factors (since $k = 0$), and therefore we have a conventional linear representation of the point group O_h. This representation may be decomposed into a sum of irreducible representations from the table above. Numerics shows that the three representations with the lowest energy are Γ_1, Γ'_{25} (in the valence band), and Γ_{15} (in the conduction band). The appearance of these

representations in the low-energy spectrum may be understood from the orbital model (see section 2.3.14).

2.3.11 Classification of states at the line $\Gamma - X$

At this line, the point group is reduced to those operations preserving the wave vector k (the so called *small point group*), i.e., preserving the direction along one of the crystallographic axes (e.g., $(1, 0, 0)$).

One can check that, since the direction is preserved, the translation in (2.3.8) contributes a phase factor, which may be compensated by putting $\alpha(g) = -\mathbf{k}\,\Delta\mathbf{x}$, where $\Delta\mathbf{x}$ is the vector of the translation L. Therefore it is again sufficient to consider the conventional representations without phase factors.

The small point group consists of only those group elements of O_h which preserve one of the faces of the cube. There are 8 such elements which fall into five classes of conjugate elements. The character table is

	1	2_{90°	1_{180°	2_+	$2_\times$
Δ_1	1	1	1	1	1
Δ_2	1	−1	1	−1	1
Δ_1'	1	1	1	−1	−1
Δ_2'	1	−1	1	1	−1
Δ_5	2	0	−2	0	0

2.3.12 Classification of states at the line $\Gamma - L$

The same argument is valid for the line $\Gamma - L$, except that now the small group only contains elements preserving the diagonal $(1, 1, 1)$. In terms of the symmetries of a cube, this group corresponds to fixing one corner of the cube.

The group has three elements and is equivalent to the group S_3 considered in the previous lecture. There are 6 elements, 3 conjugacy classes, and the representations have dimensions 1, 1, and 2.

2.3.13 Classifications of states at the points X and L

At these points, the phase factors cannot be compensated, since now the direction of the k vector may also be reversed. The classification of the states in this case requires the use of projective representations (or, equivalently, doubling the group). We do not discuss it in the lecture, but those interested may find details in the literature.

2.3.14 Symmetry classification from electron orbitals

The appearance of the representations Γ_1, Γ_{25}', and Γ_{15} in the low-energy spectrum may be understood if we assume that the relevant valence and conduction bands are mainly composed of the (hybridized) $2s$ and $2p$ orbitals of the carbon atoms. For each k vector, the linear space spanned by these orbitals is 8-dimensional (two atoms per unit cell, each atom containing one s and three p orbitals).

The symmetry analysis at the point Γ proceeds as follows: we first decompose the representation of the point group in this 8-dimensional space into irreducible representations

and then deduce the ordering of those irreducible representation by energy, based on a tight-binding description.

The point group O_h acts in the 8-dimensional space of orbitals by rotating the p orbitals and (for some of the operations) exchanging the two sublattices of atoms (the red and blue atoms in Fig. 1). Namely, the operations 6_{90°, 6_{180°, I, $I3_{180^\circ}$, and $I8_{120^\circ}$ change the orientations of the tetrahedron of the interatomic bonds around each atom and therefore must be accompanied by a translation exchanging the two sublattices. For these conjugacy classes, the character thus equals zero. For the remaining operations of the point group, the orientation of the tetrahedrons is preserved, therefore the atomic sublattices are also preserved, and the characters can be calculated from analyzing the rotation of a single atom (the s orbital always contributes 1 to the trace, while the triplet of p orbitals contributes $1 + 2\cos\alpha$, where α is the rotation angle). Thus we arrive at the following character for this 8-dimensional representation:

	1	6_{90°	3_{180°	6_{180°	8_{120°	I	$I6_{90^\circ}$	$I3_{180^\circ}$	$I6_{180^\circ}$	$I8_{120^\circ}$
Γ_{s+p}	8	0	0	0	2	0	0	0	4	0

Projecting this representation onto each of the irreducible representations, we arrive at

$$\Gamma_{s+p} = \Gamma_1 \oplus \Gamma'_{25} \oplus \Gamma'_2 \oplus \Gamma_{15} \,. \tag{2.3.9}$$

The ordering of these representations in energy can be deduced from arguments based on simple assumptions about interatomic coupling. Namely, we assume a tight-binding model with the hopping amplitudes between the nearest-neighbor atoms (i.e., between the blue and red atoms in Fig. 1) being the largest energy scale (larger than the energy difference between the orbitals $2s$ and $2p$ and larger than the next-nearest-neighbor hopping). Then we expect that, among the four representations (2.3.9), the one with the lowest energy will be Γ_1 (since its wave function does not change sign and therefore minimizes the kinetic energy). At the same time, if we only consider the nearest-neighbor hopping terms, then changing the sign of the wave function components on one of the two atomic sublattices reverses the sign of the hopping energy. Therefore, the representation Γ'_2 should be the highest one in energy. The two representations Γ'_{25} and Γ_{15} have intermediate energies, and their competition is decided by the behavior under the inversion I. The representation Γ'_{25} is even with respect to I and therefore is even on each nearest-neighbor bond, thus gaining energy from the nearest-neighbor hopping. On the other hand, Γ_{15} is odd with respect to I and therefore it loses the same amount of energy on the nearest-neighbor bonds. Thus we can predict that the order of the levels (increasing in energy) is Γ_1, Γ'_{25}, Γ_{15}, and Γ'_2. Remarkably, this order agrees with more detailed numerical calculations (Fig. 4).

3 Interacting electrons: Many-body methods

Refs: [Mar] Appendix C, [AM] Chapter 17, [BR].

3.1 Second quantization and Wick theorem

3.1.1 Bosons and fermions

Indistinguishable quantum particles can be of two types: *bosons* (the wave function is fully symmetric with respect to the permutations of particles) and *fermions* (fully antisymmetric). [In terms of the irreducible representations of the permutation group, these states belong to the trivial and "parity" representations, respectively.]

Fully symmetric and antisymmetric states may be described in terms of Hilbert spaces. Given a *single-particle* Hilbert space $\mathcal{H}$, we can construct the space of symmetrized and antisymmetrized N-particle states as symmetrized and antisymmetrized products of N copies of $\mathcal{H}$: we denote such spaces $S_\pm \mathcal{H}^{\otimes N}$, respectively. If we add together all such spaces with all possible particle numbers, we construct the bosonic/fermionic *Fock space*:

$$\mathcal{F}_\pm(\mathcal{H}) = \bigoplus_{N=0}^{\infty} S_\pm \mathcal{H}^{\otimes N} \,. \tag{3.1.1}$$

Note that the sum starts with $N = 0$ (the vacuum state). In the case of fermions, if $\mathcal{H}$ has a finite dimension m, then the spaces $S_+\mathcal{H}^{\otimes N}$ vanish for $m > N$ (so the sum is actually limited to $N \leq m$).

The symmetrization/antisymmetrization of states can be defined as

$$S_\pm(\varphi_1 \otimes \ldots \otimes \varphi_N) = \frac{1}{N!} \sum_{\sigma}^{N!} \varphi_\sigma(1) \otimes \ldots \otimes \varphi_\sigma(N) \,, \tag{3.1.2}$$

where the sum is taken over all the permutations of N elements (N states). In our discussion below, we will assume that the states φ_α are chosen from an orthonormal basis (although many of the formulas may be simply generalized to a non-orthonormal case as well).

Since the ordering of the states φ_α in the (anti)symmetrized product (3.1.2) is irrelevant, the multi-particle state may be specified by the *occupation numbers* n_α: the multiplicity of each basis state φ_α in the product (3.1.2). For fermions, the occupation number n_α can take values 0 and 1. For bosons, it can take all non-negative integer values. The states (3.1.2) for all possible sets of occupation numbers form a basis of the Fock space $\mathcal{F}_\pm(\mathcal{H})$.

The states (3.1.2) are not correctly normalized. Their normalization can be computed:

$$\|S_\pm(\varphi_1 \otimes \ldots \otimes \varphi_N)\|^2 = \frac{\prod_\alpha n_\alpha!}{N!} \,. \tag{3.1.3}$$

Therefore correctly normalized states can be defined as

$$|\varphi_1, \ldots, \varphi_N\rangle_\pm^{(n)} = \frac{\sqrt{N!}}{\prod_\alpha \sqrt{n_\alpha!}} \, S_\pm(\varphi_1 \otimes \ldots \otimes \varphi_N) \,. \tag{3.1.4}$$

This construction is completely parallel for bosons and fermions.

3.1.2 Operators of creation and annihilation

For interacting particles, one needs to operate with states in the many-particle space $S_\pm \mathcal{H}^{\otimes N}$. It turns out more practical to work with the full Fock space (3.1.1), even if the particle number N is conserved. The operators in the Fock space may be most conveniently expressed in terms of *creation* and *annihilation* operators. The creation operators are defined as (both for bosons and for fermions):

$$a_\alpha^+ |\varphi_1, \ldots, \varphi_N\rangle_\pm^{(n)} = \sqrt{n_\alpha + 1}\, |\varphi_\alpha, \varphi_1, \ldots, \varphi_N\rangle_\pm^{(n)} \tag{3.1.5}$$

in terms of the normalized states. Equivalently, the same operators may be written as

$$a_\alpha^+ S_\pm(\varphi_1 \otimes \ldots \otimes \varphi_N) = \sqrt{N+1}\, S_\pm(\varphi_\alpha \otimes \varphi_1 \otimes \ldots \otimes \varphi_N)\,. \tag{3.1.6}$$

The annihilation operators are defined as their Hermitian conjugates:

$$a_\alpha = \left(a_\alpha^+\right)^\dagger \tag{3.1.7}$$

Defined in this way, the operators a_α^+ and a_α obey the commutation (for bosons) or anticommutation (for fermions) relations:

$$[a_\alpha, a_\beta^+]_\pm = \delta_{\alpha\beta}\,, \tag{3.1.8}$$

$$[a_\alpha, a_\beta]_\pm = [a_\alpha^+, a_\beta^+]_\pm = 0\,. \tag{3.1.9}$$

The use of the creation and annihilation operators allows to reduce many of the calculations in the Fock space to algebraic manipulations with the (anti)commutation relations.

Example: In our calculations with electrons, we will use the limit of an infinite system size with the states φ_α being plane waves (parametrized by the wave vector k):

$$\varphi_k(x) = e^{ikx} \tag{3.1.10}$$

Those states are normalized to

$$\int d^3x\, \varphi_k^*(x)\varphi_{k'}(x) = (2\pi)^3 \delta(k-k')\,. \tag{3.1.11}$$

Correspondingly, the creation and annihilation operators associated with $\varphi_k(x)$ obey the (anti)commutation relations

$$[a_k, a_{k'}^+]_\pm = (2\pi)^3 \delta(k-k')\,. \tag{3.1.12}$$

By defining the Fourier transforms

$$a^+(x) = \int \frac{d^3k}{(2\pi)^3}\, e^{-ikx} a_k^+\,, \tag{3.1.13}$$

$$a(x) = \int \frac{d^3k}{(2\pi)^3}\, e^{ikx} a_k\,, \tag{3.1.14}$$

$$\tag{3.1.15}$$

the creation/annihilation operators in the coordinate space obey the relations

$$[a(x), a^+(x')]_\pm = \delta(x-x')\,. \tag{3.1.16}$$

3.1.3 One- and two-body operators in the Fock space

For any operator A acting in the single-particle space $\mathcal{H}$, we may construct the corresponding em one-particle operator $A_{(*)}$ in the Fock space $\mathcal{F}_{\pm}(\mathcal{H})$, whose action is given by the sum of the operators A acting on each particle. One can show that this operator may be written in terms of the creation and annihilation operators as

$$A_{(*)} = \sum_{ij} a_\alpha^+ A_{\alpha\beta} a_\beta \,, \tag{3.1.17}$$

where the sum is over the basis of the single-particle space $\mathcal{H}$ and $A_{\alpha\beta}$ are the matrix elements of A.

Example 1: Particle-number operator. $A = 1$ counts the particles. The total number of particles is given by

$$N = \sum_{\alpha} a_\alpha^+ a_\alpha \,. \tag{3.1.18}$$

Example 2: Free-particle Hamiltonian. The Hamiltonian of a free particle is diagonal in the momentum space: $E = \varepsilon_k$. Its counterpart in the Fock space can therefore be written as

$$H = \int \frac{d^3k}{(2\pi)^3}\, a_k^+ (\varepsilon_k - \mu) a_k \,, \tag{3.1.19}$$

where ε_k is the energy dispersion [$\varepsilon_k = \hbar^2 k^2/(2m)$ for a particle in an empty space], and μ is the chemical potential (which we usually include in the Hamiltonian in the Fock space). In the case of a quadratic spectrum, we can also rewrite the same operator in the coordinate space:

$$H = \int d^3x\, a^+(x) \left(-\frac{\hbar^2}{2m}\nabla^2 - \mu \right) a(x) \,. \tag{3.1.20}$$

A similar construction is possible for operators involving two and more particles. Consider, for example, the case of a *two-particle operator* V. It acts in the space of two particles $\mathcal{H} \otimes \mathcal{H}$. Let us denote its matrix elements by

$$V_{\alpha\beta,\gamma\delta} = \langle \varphi_\alpha \otimes \varphi_\beta | V | \varphi_\gamma \otimes \varphi_\delta \rangle \,. \tag{3.1.21}$$

Since the particles are indistinguishable, the matrix elements are invariant with respect to the permutation of the two particles:

$$V_{\alpha\beta,\gamma\delta} = V_{\beta\alpha,\delta\gamma} \,. \tag{3.1.22}$$

Then we can define the operator in the Fock space $\mathcal{F}_{\pm}(\mathcal{H})$, whose action is given by the sum of the operator V acting on *each pair of particles*. One can show that this operator may be written in the second-quantized form as

$$V_{(*)} = \frac{1}{2} \sum_{\alpha,\beta,\gamma,\delta} a_\alpha^+ a_\beta^+ V_{\alpha\beta,\gamma\delta} a_\delta a_\gamma \,. \tag{3.1.23}$$

Note the factor 1/2 (to avoid the double counting of particle pairs) and the ordering of the creation and annihilation operators (all the creation operators on the left of all the annihilation operators to avoid the self-interaction of particles).

Example: Potential interaction $V(x)$. The second-quantized form of the interaction takes the form

$$U = \frac{1}{2} \int d^3x\, d^3y\, a^+(x)\, a^+(y)\, V(x-y)\, a(y)\, a(x)\,. \tag{3.1.24}$$

3.1.4 Diagonalization of quadratic Hamiltonians

Hamiltonians quadratic with respect to the creation and annihilation operators (both bosonic and fermionic) have very remarkable properties:

1. They can be diagonalized and thus reduced to the case of noninteracting particles;

2. At any temperature, their equilibrium states obey the Wick theorem.

For the sake of generality (with a future application to superconductivity in mind), we consider the general case of a quadratic Hamiltonian

$$H = \begin{pmatrix} a^+ & a \end{pmatrix} \begin{pmatrix} H_{11} & H_{12} \\ H_{21} & H_{22} \end{pmatrix} \begin{pmatrix} a \\ a^+ \end{pmatrix}, \tag{3.1.25}$$

where H_{ij} are $N \times N$ blocks (N is the dimension of the single-particle Hilbert space).

Such a Hamiltonian can be diagonalized, i.e., brought to the form

$$H = \sum_{\alpha=1}^{N} \varepsilon_\alpha b_\alpha^+ b_\alpha + E_0 \tag{3.1.26}$$

where $\varepsilon_\alpha \geq 0$ (the energies of excitations), the operators b_α are linear combinations of a_α and a_α^+,

$$b_\alpha = u_{\alpha\beta} a_\beta + v_{\alpha\beta} a_\beta^+\,, \tag{3.1.27}$$

$$b_\alpha^+ = u_{\alpha\beta}^* a_\beta^+ + v_{\alpha\beta}^* a_\beta \tag{3.1.28}$$

obeying the same (anti)commutation relations:

$$[b_\alpha, b_\beta^+]_\pm = \delta_{\alpha\beta}\,, \tag{3.1.29}$$

$$[b_\alpha, b_\beta]_\pm = [b_\alpha^+, b_\beta^+]_\pm = 0\,. \tag{3.1.30}$$

Mathematically, in the fermionic case, such a diagonalization is always possible. In the bosonic case, one needs to require that the quadratic form (3.1.25) is positive-definite (if one treats a^+ and a as complex-conjugate numbers). Physically, any bosonic Hamiltonian must be positive-definite, since otherwise its spectrum would be unbounded from below.

We do not prove here this theorem about diagonalization: you can find a detailed proof and discussion in the book of Blaizot and Ripka [BR].

The practical algorithm for diagonalizing a quadratic Hamiltonian (3.1.25) consists in writing a linear combination (3.1.28) and then solving the eigenvalue problem

$$[H, b^+] = \varepsilon b^+\,. \tag{3.1.31}$$

Note that if the Hamiltonian conserves the number of particles (i.e., $H_{12} = H_{21} = 0$), then we can put $v = 0$, and the problem reduces to diagonalizing a single-particle Hamiltonian.

3.1.5 Wick theorem

Consider a quadratic Hamiltonian (3.1.25) (bosonic or fermionic). Then, for any set of operators $A_1, \ldots, A_M$ linear in a and a^+, at any temperature, the thermal average of the product

$$\langle A_1 \ldots A_M \rangle_T = \frac{\mathrm{tr}\left(e^{-\beta H} A_1 \ldots A_M\right)}{\mathrm{tr}\left(e^{-\beta H}\right)} \tag{3.1.32}$$

can be expressed in terms of pairwise averages:

$$\langle A_1 \ldots A_M \rangle_T = \sum (\pm 1)^\sigma \langle A_{i_1} A_{i_2} \rangle_T \ldots \langle A_{i_{M-1}} A_{i_M} \rangle_T \,, \tag{3.1.33}$$

where the sum is taken over all partitions (often called *contractions*) of the operators A_i into $M/2$ pairs. The ordering of the operators within each pair must coincide with the ordering of the operators in the left-hand side (i.e., in the above notation, $i_1 < i_2$, $i_3 < i_4$, etc.). In the fermionic case, the sign $(-1)^\sigma$ is the parity of the permutation $(1, \ldots, M) \mapsto (i_1, \ldots, i_M)$. There are no sign factors in the bosonic case.

For a proof of the Wick theorem, see the book [BR] or M. Gaudin, Nucl. Phys. **15**, 89 (1960) [in French].

Example: Wick theorem for a product of $M = 4$ operators.

$$\langle A_1 A_2 A_3 A_4 \rangle_T = \langle A_1 A_2 \rangle_T \langle A_3 A_4 \rangle_T \pm \langle A_1 A_3 \rangle_T \langle A_2 A_4 \rangle_T + \langle A_1 A_4 \rangle_T \langle A_2 A_3 \rangle_T \,. \tag{3.1.34}$$

Wick theorem can be applied for

1. Calculations of correlation functions in a free-particle system
2. Including interactions perturbatively, which leads to a diagrammatic expansion.

3.1.6 Application of the Wick theorem: density correlations of free fermions

First, let us illustrate the application of the Wick theorem with calculating the density-density correlation function $\langle n(x) n(y) \rangle$ in a free-fermion gas (without spin). The density operator may be expressed as

$$n(x) = a^+(x) a(x) \,, \tag{3.1.35}$$

which leads to the Wick-theorem result for the correlation function

$$\begin{aligned} \langle n(x) n(y) \rangle = \langle a^+(x) a(x) a^+(y) a(y) \rangle &= \langle a^+(x) a(x) \rangle \langle a^+(y) a(y) \rangle + \langle a^+(x) a(y) \rangle \langle a(x) a^+(y) \rangle \\ &= G(0)^2 - |G(x-y)|^2 + G(0) \delta(x-y) \,, \end{aligned} \tag{3.1.36}$$

where we have defined

$$G(x-y) = \langle a^+(x) a(y) \rangle \tag{3.1.37}$$

(in particular, $G(0) = n$ is the average particle density).

The contractions can be conveniently represented diagrammatically (Fig. 5). [The third delta-term in (3.1.36) is not shown: it corresponds to one particle contributing to both $n(x)$ and $n(y)$].

The "Green function" $G(x)$ has the form shown in Fig. 6. In 3D at zero temperature, it can be calculated exactly:

$$G(R) = \int \frac{d^3\mathbf{k}}{(2\pi)^3} e^{i\mathbf{k}\mathbf{R}} n_F(\varepsilon_k) = \frac{1}{2\pi^2 R^3} \left[\sin(k_F R) - (k_F R)\cos(k_F R)\right] \,. \tag{3.1.38}$$

Note that the resulting correlation function $\langle n(x)n(y)\rangle$ (Fig. 6) vanishes at $x \to y$, in agreement with the Pauli principle. It oscillates at the wave vector $2k_F$ (*Friedel oscillations*).

3.1.7 Application of the Wick theorem: perturbative energy of interaction (Hartree–Fock)

Consider now a spinless Fermi gas with the interaction (3.1.24). Let us calculate the interaction energy in a perturbative way, to the first order in V.

If we write the Hamiltonian as

$$H = H_0 + V\,, \tag{3.1.39}$$

then we can expand all the thermodynamic quantities with respect to V. The (grand-canonical) partition function (with $\beta = 1/T$)

$$Z = \operatorname{tr} e^{-\beta(H_0+V)} = \operatorname{tr} e^{-\beta H_0} - \beta \operatorname{tr} V e^{-\beta H_0} + O(V^2) = Z_0(1 - \beta\langle V\rangle_0 + O(V^2))\,. \tag{3.1.40}$$

(note that, to the first order, the noncommutativity of H_0 and V does not matter).

For the free energy (the "grand potential"), we thus find

$$\Phi = -T \ln Z = \Phi_0 + \langle V\rangle_0 + O(V^2)\,. \tag{3.1.41}$$

In other words, to the first order, the correction to the free energy equals the average interaction energy calculated in the unperturbed system. Using the Wick theorem, we can express $\langle V\rangle_0$ as the sum of two diagrams (the same as in the previous example), see Fig. 7.

The first diagram gives the classical contribution to the interaction energy:

$$\delta\Phi_1 = \frac{1}{2}\iint dx\,dy\,\langle n(x)\rangle V(x-y)\langle n(y)\rangle = \mathcal{V}\frac{n^2}{2}\int dx\,V(x) = \mathcal{V}\frac{n^2}{2}V_{k=0}\,, \tag{3.1.42}$$

where $\mathcal{V}$ is the total volume of the system.

The second diagram is of the exchange type:

$$\delta\Phi_2 = -\frac{1}{2}\iint dx\,dy\,G(x-y)V(x-y)G(y-x) = -\frac{\mathcal{V}}{2}\iint \frac{d^3k}{(2\pi)^3}\frac{d^3k'}{(2\pi)^3}n_k n_{k'}V_{k-k'}\,. \tag{3.1.43}$$

The correction (3.1.43) may be interpreted as a renormalization of energy of each particle by interaction. The correction to the energy of a particle at the momentum k is then

$$\delta\varepsilon_k = -\int \frac{d^3k'}{(2\pi)^3}n_{k'}V_{k-k'}\,. \tag{3.1.44}$$

As we will see later, this correction to the energy corresponds to the Hartree–Fock approximation.

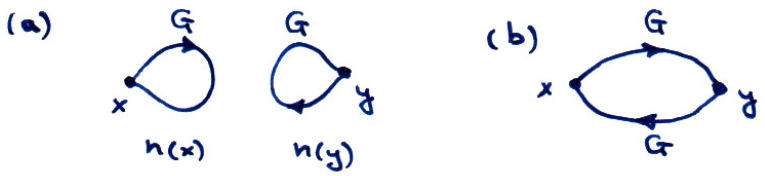

Figure 5: Two diagrams contributing to the correlation function $\langle n(x)n(y)\rangle$.

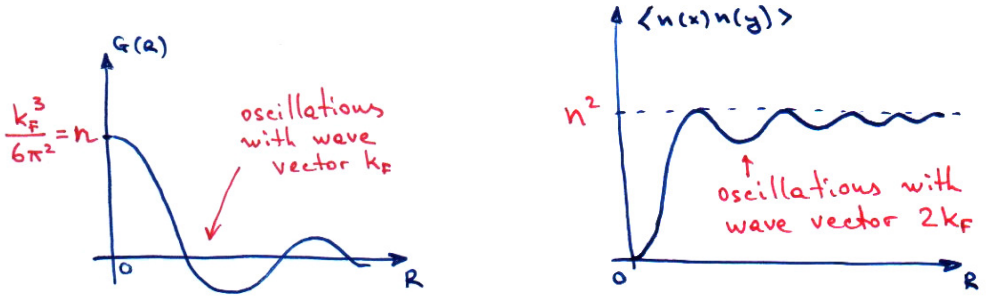

Figure 6: Qualitative sketches of $G(R)$ and $\langle n(x)n(y)\rangle$.

3.2 Introduction to Green's functions

Green's functions appear naturally in many perturbative calculations. We have seen an example in Sections 3.1.6 and 3.1.7, where $\langle a^+(x)a(y)\rangle$ may be interpreted as *equal-time* Green's functions. However, if we choose to extend the calculations of Section 3.1.7 to higher orders in interaction, we would need to introduce time-dependent (or frequency-dependent) Green's functions. Indeed, at higher orders, we cannot neglect noncommutativity between H and V in Eq. (3.1.40). The expansion of the operator exponent, to any order, is given by:

$$e^{-\beta(H_0+V)} = e^{-\beta H_0} + \int_0^\beta d\tau_1\, e^{-(\beta-\tau_1)H_0}(-V)e^{-\tau_1 H_0} + \iint_{0<\tau_1<\tau_2<\beta} d\tau_1\, d\tau_2\, e^{-(\beta-\tau_2)H_0}(-V)e^{-(\tau_2-\tau_1)H_0}(-V)e^{-\tau_1 H_0} + \dots \quad (3.2.1)$$

The same type of formula is also valid for time evolution in quantum mechanics (by replacing imaginary time τ by real time t):

$$e^{-it(H_0+V)} = e^{-itH_0} + \int_0^t dt_1\, e^{-i(t-t_1)H_0}(-iV)e^{-it_1 H_0} + \iint_{0<t_1<t_2<t} dt_1\, dt_2\, e^{-i(t-t_2)H_0}(-iV)e^{-i(t_2-t_1)H_0}(-iV)e^{-it_1 H_0} + \dots \quad (3.2.2)$$

This series can be conveniently represented graphically (Fig. 8). It has the meaning of the interaction intervening at the moments t_1, t_2, etc. during the evolution of the system.

Figure 7: Two diagrams contributing to the perturbative interaction energy: (a) Hartree contribution; (b) exchange contribution.

3.2.1 Green's functions in quantum mechanics

Before introducing Green's functions in the second-quantized formalism, we discuss briefly their application in quantum mechanics. We define the Green's function as the propagator (evolution operator)

$$G(x', x, t) = -i\langle x'|e^{-itH}|x\rangle\,\theta(t)\,, \tag{3.2.3}$$

where $\theta(t) = 1$ for $t > 0$ and $\theta(t) = 0$ for $t < 0$ (the factor $-i$ is introduced for convenience to simplify further formulas). Such a definition is usually called the *retarded* Green's function. The Green's function can be represented either in the coordinate or in the momentum space (related by a Fourier transformation) and either in the time or in the frequency space (again, related by a Fourier transformation). For example, passing to the frequency representation gives

$$G_\omega(x', x) = \int dt\, e^{i(\omega+i0)t} G(x', x, t) = \langle x'|\frac{1}{\omega - H + i0}|x\rangle\,. \tag{3.2.4}$$

If H is a free-particle Hamiltonian ($H = \varepsilon_k$ in the momentum representation), then it is convenient to represent the Green's function also in the momentum representation, where it becomes diagonal:

$$G_\omega(k', k) = \iint d^3x'\, d^3x\, G_\omega(x', x) e^{-ik'x'+ikx} = (2\pi)^3\delta(k - k')\, G_\omega(k)\,, \tag{3.2.5}$$

where

$$G_\omega(k) = \frac{1}{\omega - \varepsilon_k + i0}\,. \tag{3.2.6}$$

The appearance of such Green's functions can be understood already from the perturbation theory in quantum mechanics. If we consider a Schroedinger equation with a perturbation:

$$(H_0 + V)\Psi = E\Psi\,, \tag{3.2.7}$$

then we may formally solve it perturbatively by rewriting

$$\Psi = (E - H_0)^{-1} V\Psi\,. \tag{3.2.8}$$

The inverse $(E - H_0)^{-1}$ coincides with our above definition of the Green's function: we can also write it as an operator

$$G = \frac{1}{E - H_0 + i0} \tag{3.2.9}$$

The perturbative series for Ψ can be constructed iteratively

$$\Psi = \Psi_0 + \Psi_1 + \ldots \tag{3.2.10}$$

Figure 8: Perturbation series for the Green's function.

starting with Ψ_0 (an eigenstate of H_0 at energy E) and solving iteratively:

$$(E - H_0)\Psi_{n+1} = V\Psi_n \qquad \Rightarrow \qquad \Psi_{n+1} = (E - H_0)^{-1} V \Psi_n \,. \tag{3.2.11}$$

As a result, we get the perturbative series

$$\Psi = (1 + GV + GVGV + \ldots)\,\Psi_0 \,, \tag{3.2.12}$$

where we again recognize the series of the type shown in Fig. 8.

Yet another way to obtain the same series is to expand the full Green's function:

$$\begin{aligned} \tilde{G} &= \frac{1}{E - (H_0 + V)} \\ &= \frac{1}{E - H_0} + \frac{1}{E - H_0}\, V \, \frac{1}{E - H_0} + \frac{1}{E - H_0}\, V \, \frac{1}{E - H_0}\, V \, \frac{1}{E - H_0} + \ldots \,, \end{aligned} \tag{3.2.13}$$

which is the operator counterpart of the usual power series:

$$\frac{1}{a - \epsilon} = \frac{1}{a} + \frac{1}{a^2}\,\epsilon + \frac{1}{a^3}\,\epsilon^2 + \ldots \tag{3.2.14}$$

(Note: the order of operators in the right-hand side of (3.2.13) is important!) We can see that it again reduces to the same series in Fig. 8.

3.2.2 Application: Density-of-states oscillations around an impurity

Consider the experiment described in the paper K. Kanisawa et al, Phys. Rev. Lett. **86**, 3384 (2001): the local density of states at a given energy is measured around an impurity in a two-dimensional electron gas (Fig. 9). We can express this local density of states in terms of the retarded Green's function as

$$\rho_\omega(x) = -\frac{1}{\pi}\,\mathrm{Im}\,\tilde{G}_\omega(x, x) \,, \tag{3.2.15}$$

where $\tilde{G}$ is the full Green's function (3.2.13) To the first order in the impurity potential $V(x)$, the distortion of the local density of states is given by

$$\delta\rho_\omega(x) = -\frac{1}{\pi}\,\mathrm{Im} \int d^2y\, G_\omega(x, y)\, V(y)\, G_\omega(y, x) \,. \tag{3.2.16}$$

By approximating the potential to be a delta function $V(y) = V_0\,\delta(y)$, we find

$$\delta\rho_\omega(R) = -\frac{V_0}{\pi}\,\mathrm{Im}[G_\omega(R)]^2 \,, \tag{3.2.17}$$

where $R = |x|$ is the distance from the impurity. The Green's function of a free particle, in turn, can be expressed as

$$G_\omega(x) = \int \frac{1}{\omega - (k^2/2m) + i0}\, e^{ikx}\, \frac{d^2k}{(2\pi)^2} \,. \tag{3.2.18}$$

The two last equations solve the problem in principle. The analytic treatment of integrals is complicated in 2D, but we can simplify it in the limit $k_\omega R \gg 1$, where

Figure 9: Left: A sketch of the experimental observation in the paper of Kanisawa et al. Friedel oscillations of the local density of states are observed around impurities. x is the observation point, y is the position of the impurity. Right: the diagram representing the first-order correction to the density of states due to the impurity potential.

$k_\omega = (2m\omega)^{1/2}$. Performing first the integrals over the angular degrees of freedom in (3.2.18), we find

$$G_\omega(R) = \int_0^\infty \frac{kJ_0(kR)}{\omega - (k^2/2m) + i0} \frac{dk}{2\pi}\,, \tag{3.2.19}$$

where J_0 is the Bessel function:

$$J_0(x) = \int_0^{2\pi} \frac{d\varphi}{2\pi} e^{ix\cos\varphi}\,. \tag{3.2.20}$$

At $kR \gg 1$, the asymptotic behavior of $J_0(kR)$ is

$$J_0(kR) \approx \sqrt{\frac{2}{\pi kR}} \cos\left(kR - \frac{\pi}{4}\right) \tag{3.2.21}$$

The main contribution to the integral (3.2.19) comes from the pole at $k = k_\omega$ and can be extracted by representing the cosine as a sum of two oscillating exponents. As a result, we get

$$G_\omega(R) \approx -\frac{im}{\sqrt{2\pi k_\omega R}} e^{i(k_\omega R - \pi/4)} \tag{3.2.22}$$

and, finally,

$$\delta\rho_\omega(R) = -\frac{m^2 V_0}{2\pi^2 k_\omega R} \cos(2k_\omega R)\,. \tag{3.2.23}$$

These Friedel oscillations have the same nature as those in the density correlations $\langle n(x)n(y)\rangle$ studied in Section 3.1.6, although the Green's functions are different in these two problems: equal-time ($t = 0$) vs. fixed-frequency).

3.2.3 Green's functions in many-body problems (at zero temperature)

Now we extend the Green's-function approach to many-body problems using the expansion (3.2.2) and the Wick theorem (see Section 3.1.5) In the expansion (3.2.2), we encounter products of creation and annihilation operators with the evolution operators $\exp(-itH_0)$ inserted between them. It will be therefore convenient to define the time-dependent operators

$$a(t) = e^{itH} a e^{-itH}\,, \qquad a^+(t) = e^{itH} a^+ e^{-itH}\,, \tag{3.2.24}$$

where H may be either the full Hamiltonian or the quadratic Hamiltonian H_0, depending on the situation.

Note that in the case of a *quadratic Hamiltonian*, $a(t)$ and $a^+(t)$ always remain linear combinations of the original creation and annihilation operators a and a^+. Proof: they obey the linear equations of motion

$$\dot{a}(t) = i[H_0, a(t)] \tag{3.2.25}$$

[and similarly for $a^+(t)$], so if $a(t)$ is linear in a and a^+ at some moment t, it will remain linear at the "next" moment, too. From the linearity property, it follows that $a(t)$ and $a^+(t)$ obey the Wick theorem.

Now we are ready to introduce the time-dependent Green's functions $\langle a^+(t_1)a(t_2)\rangle$. More precisely, we introduce three different Green's functions:

- the *retarded* Green's function:

$$G^R(t_1 - t_2; x_1, x_2) = -i\langle\{a(t_1, x_1), a^+(t_2, x_2)\}\rangle\theta(t_1 - t_2)\,; \tag{3.2.26}$$

- the *advanced* Green's function:

$$G^A(t_1 - t_2; x_1, x_2) = i\langle\{a(t_1, x_1), a^+(t_2, x_2)\}\rangle\theta(t_2 - t_1)\,; \tag{3.2.27}$$

- the *causal* (or time-ordered) Green's function:

$$G^c(t_1 - t_2; x_1, x_2) = -iT\langle a(t_1, x_1)a^+(t_2, x_2)\rangle\,, \tag{3.2.28}$$

  where T denotes time ordering:

$$T\,A(t_1)B(t_2) = \begin{cases} A(t_1)B(t_2) & \text{if } t_1 > t_2 \\ -B(t_2)A(t_1) & \text{if } t_2 > t_1 \end{cases} \tag{3.2.29}$$

(we assumed that the operators a and a^+ are fermionic; for bosonic operators, there is no sign change when permuting them).

The above Green's functions may be defined either for the quadratic part of the Hamiltonian H_0 (with the time evolution by H_0 and average taken over the ground state of H_0) or for the full Hamiltonian. As before, we will denote the Green's functions defined for the full Hamiltonian by tildes, while the Green's function for the quadratic part written without additional marks.

In the general case, we can establish the following relations between these Green's functions:

$$\tilde{G}^R_\omega(k) = [\tilde{G}^A_\omega(k)]^* \tag{3.2.30}$$

$$\tilde{G}^c_\omega(k) = \begin{cases} \tilde{G}^R_\omega(k)\,, & \omega > 0 \\ \tilde{G}^A_\omega(k)\,, & \omega < 0\,. \end{cases} \tag{3.2.31}$$

(here ω is measured from the chemical potential μ or, equivalently, μ is included in the Hamiltonian).

In the case of a quadratic Hamiltonian, more properties hold:

- In the definitions of G^R and G^A we may remove the averaging $\langle \ldots \rangle$, since the anticommutators are just numbers, not operators. In other words, G^R and G^A do not depend on the many-particle state, but are single-particle properties.

- G^R coincides with the quantum-mechanical Green's function (as can be seen from considering its definition in the vacuum state).

- For the free-particle Hamiltonian, we can find

$$G^R(\omega, k) = \frac{1}{\omega - (\varepsilon_k - \mu) + i\delta} \tag{3.2.32}$$

$$G^A(\omega, k) = \frac{1}{\omega - (\varepsilon_k - \mu) - i\delta} \tag{3.2.33}$$

$$G^c(\omega, k) = \frac{1}{\omega - (\varepsilon_k - \mu) + i\delta \operatorname{sign} \omega} \tag{3.2.34}$$

  In other words, in the ω-k representation, G^R, G^A, and G^c differ only by the regularization of the poles: G^R corresponds to all states empty, G^A to all states occupied, and G^c keeps track of the occupation number being 0 or 1.

The time-ordered Green's function G^c turns out to be useful for the diagrammatic technique, since the expansion (3.2.2) naturally produces time-ordered correlation functions. Note also that the Wick theorem can be reformulated for time-ordered products, since time ordering guarantees the same order of operators in the left and right-hand sides of (3.1.33). At the same time, the Green's function $\tilde{G}^c$ can be used to express single-particle average quantities. The poles of the Green's functions correspond to the spectrum of excitations (the poles above and below the real axis of ω correspond to hole and electron excitations, respectively).

3.2.4 Diagrammatic expansion of a single Green's function

Let us illustrate the diagrammatic approach with a perturbative expansion of a single Green's function. In other words, we would like to express the full Green's function $\tilde{G}^c$ in terms of the bare Green's function G^c and the interaction parameters. We assume that the Hamiltonian has the usual form

$$H = H_0 + V\,, \tag{3.2.35}$$

where the quadratic Hamiltonian H_0 is the free-fermion one (3.1.19) and the interaction V is a pairwise potential interaction (3.1.24).

The Green's function (3.2.28) involves interaction both in the time-evolution part between the moments t_1 and t_2 and in the ground state over which we average. To treat them on equal footing, we express the ground state as a result of an "adiabatic switching" of the interaction:

$$|\Psi_0\rangle = e^{-iH(0-t_{-\infty})}|\Psi_\infty\rangle\,, \tag{3.2.36}$$

where the perturbative expression is assumed to switch on adiabatically (or the time is assumed to have a small imaginary part), so that the ground state is selected after a sufficiently slow evolution. The starting time $t_{-\infty}$ will be taken to $-\infty$ at the end of the

calculation. The starting state $|\Psi_\infty\rangle$ is the ground state of the unperturbed Hamiltonian H_0. Then we can represent the Green's function (3.2.28) as (we put $t_1 > t_2$, to be specific):

$$\tilde{G}^c(t_1 - t_2; x_1, x_2) = -i \, \frac{\langle \Psi_\infty | e^{-iH(t_\infty - t_1)} a(x_1) e^{-iH(t_1 - t_2)} a^+(x_2) e^{-iH(t_2 - t_{-\infty})} | \Psi_\infty \rangle}{\langle \Psi_\infty | e^{-iH(t_\infty - t_{-\infty})} | \Psi_\infty \rangle} \,. \quad (3.2.37)$$

The evolution operators in both the numerator and the denominator can now be expanded in V by writing $H = H_0 + V$ and using the expansion (3.2.2). Then the result can be expressed in terms of products of the unperturbed Green's functions G^c by using the Wick theorem. Each of these terms can be represented as a diagram.

An important observation (which can be proven by a combinatoric counting): disconnected loops of the diagrams in the numerator are exactly canceled by the diagrams from the denominator! So the actual sum must include only connected diagrams.

3.2.5 Hartree–Fock as a renormalization of the Green's function

To the first order in V, the procedure described above produces two diagrams shown in Fig. 10. The integrals corresponding to these diagrams are:

$$\delta_1 \tilde{G}^c(t_1 - t_2; x_1, x_2) = \iiint dx \, dy \, dt \, V(x-y) \, n(y) \, G^c(t_1 - t; x_1, x) \, G^c(t - t_2; x, x_2) \,, \quad (3.2.38)$$

where $n(y) = -iG^c(\Delta t = -0; y, y)$ is the average particle density at point y (in the uniform case, it is simply the average density n), and

$$\delta_2 \tilde{G}^c(t_1 - t_2; x_1, x_2) = i \iiint dx \, dy \, dt \, V(x-y) \times G^c(t_1 - t; x_1, x) \, G^c(\Delta t = -0; x, y) \, G^c(t - t_2; y, x_2) \,. \quad (3.2.39)$$

We can also rewrite the same integrals in the frequency-momentum representation (in the translationally invariant case):

$$\delta_1 \tilde{G}^c_\omega(k) = V_{k=0} \, n \, [G^c_\omega(k)]^2 \,, \quad (3.2.40)$$

$$\delta_2 \tilde{G}^c_\omega(k) = i \int \frac{d^3k'}{(2\pi)^3} \left[\int \frac{d\omega}{2\pi} \, e^{i\omega 0} \, G^c_\omega(k') \right] V_{k-k'} [G^c_\omega(k)]^2 \,. \quad (3.2.41)$$

The factor $e^{i\omega 0}$ indicates that we have to close the integration contour in the upper half plane:

$$G^c(\Delta t = -0; k') = \int \frac{d\omega}{2\pi} \, e^{i\omega 0} \, G^c_\omega(k') = i n_{k'} \quad (3.2.42)$$

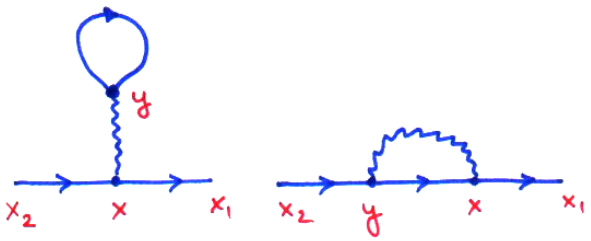

Figure 10: The two leading corrections to the Green's function due to interaction.

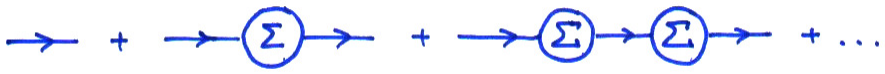

Figure 11: The geometric series (3.2.43). Σ denotes the "irreducible" part of the expansion.

is simply the occupation number at the momentum k.

Now we remark that these are in fact corrections to the *denominator* of the Green's function. Indeed, if we know the irreducible *self-energy* part (i.e., the part which cannot be disconnected by breaking any single Green's-function line), then we can sum the series [compare with (3.2.13)]:

$$G^c_\omega(k) + G^c_\omega(k)\Sigma_\omega(k)G^c_\omega(k) + G^c_\omega(k)\Sigma_\omega(k)G^c_\omega(k)\Sigma_\omega(k)G^c_\omega(k) + \ldots = \frac{1}{\omega - (\varepsilon_k - \mu + \Sigma_\omega(k)) + i\delta\,\mathrm{sign}\,\omega} \tag{3.2.43}$$

(see Fig. 11). In our case, this means that we can interpret the corrections (3.2.40) and (3.2.41) as corrections to the energy

$$\delta\varepsilon_k = \Sigma_\omega(k) = n\,V_{k=0} - \int \frac{d^3k'}{(2\pi)^3} n_{k'}\,V_{k-k'}\,, \tag{3.2.44}$$

which reproduces our earlier result (3.1.44).

Moreover, if we assume that the chemical potential is controlled by the overall density of particles and is not renormalized by the interaction (which is the case in the metal), then our calculation amounts, in fact, to summing a large number of diagrams, which can be written in a recursive way in Fig. 12. Some diagrams are, however, not included (Fig. 13), in particular those responsible for screening.

3.2.6 Hartree–Fock as a variational method

Ref: [AM] Chapter 17.

The same Hartree–Fock approximation may also be understood as a variational procedure. Suppose that we look for a Slater-determinant state

$$\Psi = S_-(\varphi_1 \otimes \ldots \otimes \varphi_N) \tag{3.2.45}$$

with the lowest variational energy. The variational parameters are the single-particle states $\varphi_1, \ldots, \varphi_N$. These states are optimized to minimize the expectation value $\langle\Psi|H|\Psi\rangle$

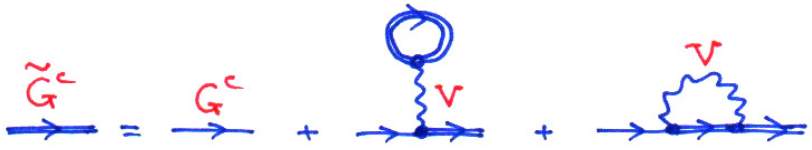

Figure 12: The recursive equation for the Hartree–Fock sum.

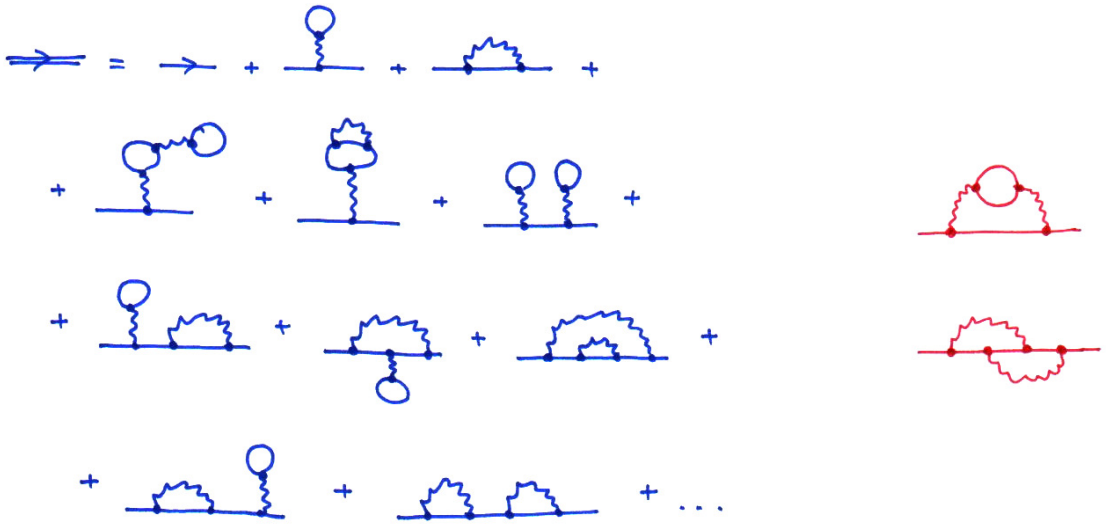

Figure 13: Left: the diagram included in the Hartree–Fock series recursively defined in Fig. 12. Right: two second-order diagrams not included in this series.

of the Hamiltonian

$$H = \sum_{i=1}^{N} \left[-\frac{1}{2m}\nabla^2 + U(x_i) \right] + \frac{1}{2}\sum_{i\neq j} U(x_i - x_j) \tag{3.2.46}$$

under the normalization condition $\langle\Psi|\Psi\rangle = 1$. Without loss of generality, we may assume the single-particle states φ_i to be orthonormal, and then the normalization condition may be reduced to fixing the normalization of each of the single-particle states $\langle\varphi_i|\varphi_i\rangle = 1$. This would lead to introducing N Lagrange multipliers for each of these conditions.

The expectation value of the Hamiltonian may be shown to be given by

$$\begin{aligned}\langle\Psi|H|\Psi\rangle = \sum_{i=1}^{N}\langle\varphi_i| -\frac{1}{2m}\nabla^2 + U|\varphi_i\rangle \\ + \frac{1}{2}\sum_{i,j}\iint dx\,dy\,|\varphi_i(x)|^2\,|\varphi_j(x)|^2\,U(x-y) \\ - \frac{1}{2}\sum_{i,j}\iint dx\,dy\,\varphi_i^*(x)\varphi_j(x)\varphi_j^*(y)\varphi_i(y)\,U(x-y)\,,\end{aligned} \tag{3.2.47}$$

which is nothing else but the Wick theorem for the Slater-determinant state (3.2.45). Its variation leads to a set of nonlinear equations that need to be solved self-consistently:

$$\left(-\frac{1}{2m}\nabla^2 + U + \Sigma\right)\varphi_i = \varepsilon_i\varphi_i\,, \tag{3.2.48}$$

where

$$[\Sigma\varphi_i](x) = \int dy\,n(y)\,U(x-y)\,\varphi_i(x) - \sum_j \int dy\,\varphi_j(x)\varphi_j^*(y)\varphi_i(y)\,U(x-y) \tag{3.2.49}$$

and

$$n(y) = \sum_j |\varphi_j(y)|^2 \,. \tag{3.2.50}$$

Note the resemblance of these formulas to the diagrammatic expression in Fig. 12 [eqs. (3.2.38) and (3.2.39)] for the self-energy Σ. In fact, this correspondence is exact, if we relate the Green's function to the single-particle states

$$G^c_\omega(x,y) = \sum_i \frac{\varphi_i(x)\varphi_i^*(y)}{\omega - (\varepsilon_i - \mu) + i\delta\,\mathrm{sign}\,\omega} \,, \tag{3.2.51}$$

where the sum is taken over all (empty and occupied) states. The equal-time Green's function is then

$$G^c(\Delta t = -0; x, y) = \sum_{i=1}^{N} \varphi_i(x)\varphi_i^*(y) \,, \tag{3.2.52}$$

with the sum taken over the N occupied states. The Lagrange multipliers ε_i in the variational approach correspond to the single-particle energies in the Hartree-Fock approximation.

In other words, the variational procedure is exactly equivalent to the diagrammatic approximation described in the previous section.

The Hartree–Fock approximation may be used for calculating the electronic structure of solids and molecules. However, its mean-field nature (neglecting

correlations between electrons of opposite spins) makes the results not very accurate, and other more efficient approximations (such as density-functional theory) are more commonly used.

3.3 Screening of Coulomb interactions in a metal

Ref: [AM] Chapter 17.

As we saw in the previous sections, the Hartree–Fock approximation does not include any screening of long-range Coulomb interactions. As a particular consequence of this neglect, the spectrum of excitations near the Fermi surface gets, within the Hartree–Fock approximation, an unphysical logarithmic singularity. This problem can be repaired by including screening.

In this section, we discuss screening at the linear-response level in the static situation (no time dependence). Namely, we assume a small probe charge Q at the position $x = 0$ and calculate the resulting electrostatic potential $\phi(r)$ around this charge.

In the absence of screening, the potential is

$$\phi^{\mathrm{ext}}(R) = \frac{Q}{R} \tag{3.3.1}$$

The screening results from a redistribution of the electronic density due to the potential, which, in turn, itself changes the potential. In other words, the potential and the density distribution need to be calculated self-consistently.

The response of the density to the potential can be written in the momentum representation as

$$\delta n(q) = \chi(q)\, e\phi(q) \,. \tag{3.3.2}$$

On the other hand, the feedback of the density modulation on the potential is given by the Gauss equation

$$-\frac{1}{4\pi}\nabla^2\phi(x) = Q\,\delta(x) + e\,\delta n(x)\,, \tag{3.3.3}$$

which, in the momentum representation takes the form

$$\frac{q^2}{4\pi}\phi(q) = Q + e\,\delta n(q) \tag{3.3.4}$$

Putting the two equations together, we find

$$\phi(q) = \frac{Q}{\frac{q^2}{4\pi} - e^2\,\chi(q)}\,. \tag{3.3.5}$$

The Fourier transform of this function gives the screened interaction potential $\phi(r)$.

3.3.1 Thomas–Fermi theory of screening

The simplest approximation we can make is to assume that all the coordinate dependencies are slow and calculate the response (3.3.2) in the static approximation (which amounts to putting $q = 0$). Then we immediately find

$$\chi(q{=}0) = -\nu_0\,, \tag{3.3.6}$$

the density of states at the Fermi level (including spin degeneracy),and

$$\phi(q) = \frac{4\pi Q}{q^2 + \kappa^2}\,, \tag{3.3.7}$$

where

$$\kappa = (4\pi e^2\nu_0)^{1/2}\,. \tag{3.3.8}$$

The Fourier transform of this potential gives

$$\phi(R) = \frac{Q}{R}\,e^{-\kappa R}\,, \tag{3.3.9}$$

i.e., κ^{-1} has the meaning of the screening length.

3.3.2 Lindhard theory of screening

A more accurate approximation is to calculate the response (3.3.2) within the free-fermion gas model. This was, in fact, done in the problem 7.2, and the answer reads

$$\chi(R) = -i\int\frac{d\omega}{2\pi}[G^c_\omega(R)]^2\,. \tag{3.3.10}$$

To convert this result into the screened potential, we need to Fourier transform $\chi(r) \mapsto \chi(q)$, substitute into eq. (3.3.5) and Fourier transform back to the real space.

An exact calculation for the free 3D gas (without spin) gives

$$G^c_\omega(R) = -\frac{m}{2\pi R}\,e^{i(\mathrm{sign}\,\omega)k_\omega r}\,, \tag{3.3.11}$$

Figure 14: RPA series for screening.

where $k_\omega = [2m(\mu+\omega)]^{1/2}$,

$$\chi(R) = -\frac{m}{16\pi^3 R^4}\left[\sin(2k_F R) - (2k_F R)\cos(2k_F R)\right], \tag{3.3.12}$$

and

$$\chi(q) = -\frac{mk_F}{2\pi^2} F\left(\frac{q}{2k_F}\right), \tag{3.3.13}$$

where

$$F(\alpha) = \frac{1}{2} + \frac{1-\alpha^2}{4\alpha}\ln\left|\frac{1+\alpha}{1-\alpha}\right|. \tag{3.3.14}$$

For the spinful case, the results for $\chi(R)$ and $\chi(q)$ must be multiplied by 2 (for the two spin components).

We see that at $q = 0$ it reproduces the Thomas–Fermi approximation. Thus the long-range $1/r$ part is screened in exactly the same way as described above (at the scale κ^{-1}). At the same time, the logarithmic singularity in (3.3.13) may be shown to give rise to the oscillating contribution

$$\phi(R) \propto \frac{1}{R^3}\cos(2k_F R). \tag{3.3.15}$$

3.3.3 Diagrammatic interpretation of the Lindhard theory

We can also obtain the Lindhard theory by simply summing the diagrammatic series in Fig. 14. Each loop corresponds to $\chi(R)$ as given by (3.3.10) while each wavy line corresponds to the bare potential

$$V_0(R) = \frac{e^2}{R} \qquad \Rightarrow \qquad V_0(q) = \frac{4\pi e^2}{q^2}. \tag{3.3.16}$$

Summing up the geometric series gives

$$\begin{aligned} V(q) = V_0(q) + V_0(q)\,\chi(q)\,V_0(q) + V_0(q)\,\chi(q)\,V_0(q)\,\chi(q)\,V_0(q) + \ldots \\ = \frac{V_0(q)}{1-\chi(q)\,V_0(q)}, \end{aligned} \tag{3.3.17}$$

which exactly reproduces the result of the Lindhard theory.

This type of approximation (corresponding to the summation of the series shown in Fig. 14) is also frequently called *random phase approximation* (RPA). It can also be extended to include dynamic screening (and plasmon excitations) by considering this series at a finite frequency (our calculation only considered the zero-frequency limit).

4 Phonons. Electron-phonon interaction

Refs: [AM] Chapter 23, [PC] Section 9.7.

Phonons are vibrations of a crystal lattice. They can be viewed as bosonic particles which propagate through the crystal and interact with electrons. In this section, we review some basic properties of phonons and show that interaction with phonons produces attraction between electrons (which is the mechanism of superconductivity in most superconductors).

4.1 Harmonic oscillators as free bosons

Any harmonic oscillator may be viewed as a single bosonic mode, which may be occupied by 0, 1, 2, etc. bosons. Consider the quantum Hamiltonian

$$H = \frac{p^2}{2m} + K\frac{q^2}{2} \tag{4.1.1}$$

with the operators p and q satisfying the canonical commutation relations $[p, q] = -i$ (Planck constant is put to 1, as usual). Then the operators

$$\begin{aligned} b &= \frac{1}{\sqrt{2}}\left[q(Km)^{1/4} + i\frac{p}{(Km)^{1/4}}\right], \\ b^+ &= \frac{1}{\sqrt{2}}\left[q(Km)^{1/4} - i\frac{p}{(Km)^{1/4}}\right] \end{aligned} \tag{4.1.2}$$

obey the canonical bosonic commutation relations

$$[b, b^+] = 1\,, \tag{4.1.3}$$

and the Hamiltonian takes the form

$$H = \omega\left(b^+b + \frac{1}{2}\right) = \omega\left(n + \frac{1}{2}\right), \tag{4.1.4}$$

where $\omega = (K/m)^{1/2}$ is the oscillator frequency (= energy, once $\hbar = 1$) and n is the number of *bosons*.

4.2 Phonons

The definition of phonons is similar to the one-dimensional example above. In a crystal with N ions, the vibrations of the lattice can be parametrized by $3N$ coordinates (displacements of ions) and $3N$ momenta. Small vibrations can be described by a quadratic Hamiltonian, which is a $3N$-dimensional version of (4.1.1). This Hamiltonian can be diagonalized, and its eigenmodes decoupled. Because of the translational symmetry of the lattice, the eigenmodes can be labeled by the wave vector (just like electron bands). If the crystal lattice has M atoms per unit cell, the number of bands (the number of phonon states for each k vector) equals $3M$.

The phonon Hamiltonian takes the quadratic form

$$H = \sum_{k,\alpha} \omega_{k,\alpha} b^+_{k,\alpha} b_{k,\alpha} \tag{4.2.1}$$

(we have dropped the constant ground-state energy). The index α labels the phonon bands. At the level of the harmonic approximation, phonons do not interact. Anharmonic terms would correspond to phonon-phonon interactions.

There are three phonon modes which are special: the *acoustic* phonons. They correspond to slowly varying displacement of atoms and have a linear dispersion relation

$$\omega_k = c|k| \quad \text{as} \quad k \to 0\,. \tag{4.2.2}$$

The energy of the acoustic phonons tends to zero as $k \to 0$. In this limit, all displacements are equal, which corresponds to displacing crystal as a whole, which obviously does not cost any energy. The sound velocities c for the longitudinal and transverse sounds are generally different and may also depend on the direction.

The phonons have energy bands which are periodic functions of k. They extend between 0 and some characteristic energy scale, the so called *Debye energy* ω_D. By the order of magnitude,

$$\omega_D \sim c/a_0 \tag{4.2.3}$$

(where a_0 is the lattice constant), which is much less than the Fermi energy $\varepsilon_F \sim v_F/a_0$. The typical Debye energy in a metal is between 100 K and 500 K (as opposed to the Fermi energy of about 10^4 K).

4.3 Specific heat of phonons

Except at very low temperatures, phonons give the main contribution to the specific heat. To calculate the specific heat of phonons exactly, one needs to know the distribution of phonon modes over energies [i.e., the *density of states* $\nu_{\rm ph}(\omega)$].

For low-temperature specific heat (when only low-energy phonons are excited), the behavior of at $\omega \to 0$ matters, while for the high-temperature limit, it is important that the phonons have an upper cut-off in energy at $\omega \sim \omega_D$. The simplest approximation accurate in both limits is the *Debye theory*:

$$\nu_{\rm ph}(\omega) = \begin{cases} C\,\omega^2\,, & \omega < \omega_D\,, \\ 0\,, & \omega > \omega_D \end{cases} \tag{4.3.1}$$

(see Fig. 15a). The constant C is fixed by the total number of modes

$$C\int_0^{\omega_D} \omega^2 d\omega = 3N \qquad \Rightarrow \qquad C = \frac{9N}{\omega_D^3}\,, \tag{4.3.2}$$

where N is the total number of atoms in the crystal. The specific heat of one bosonic mode with energy ω can be found as

$$c_V(\omega) = \frac{\partial E}{\partial T} = \omega\,\frac{\partial}{\partial T}\,\frac{1}{e^{\omega/T}-1} = \frac{\omega^2}{T^2}\,\frac{e^{\omega/T}}{(e^{\omega/T}-1)^2}\,. \tag{4.3.3}$$

So the total specific heat is

$$C_V = \int_0^\infty c_V(\omega)\nu_{\rm ph}(\omega)d\omega = 3N\,f\left(\frac{T}{\omega_D}\right)\,, \tag{4.3.4}$$

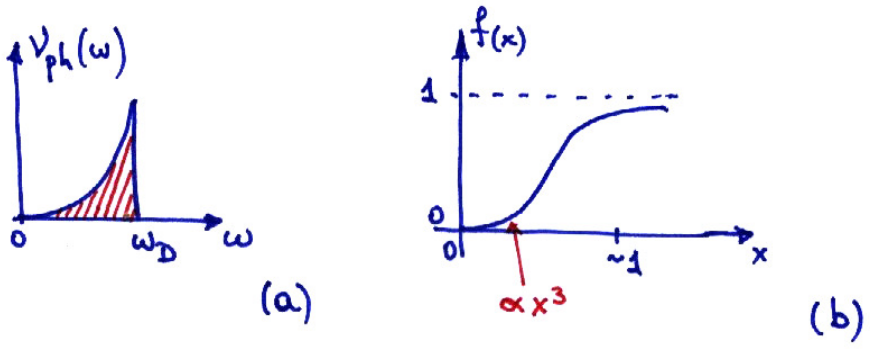

Figure 15: **(a)**: Ansatz for $\nu_{\rm ph}(\omega)$ in the Debye theory; **(b)**: The form of the function $f(x)$ in Eq. (4.3.4).

where

$$f(x) = 3x^3 \int_0^{1/x} \frac{y^4 e^y}{(e^y - 1)^2}\, dy \tag{4.3.5}$$

is a universal function (Fig. 15b).

This approximation describes a large number of different materials remarkably well (with one fitting parameter ω_D). At low temperatures, $C_V \propto T^3$ (the black-body specific heat), while at high temperatures $C_V \to 3N$ (the classical specific heat of $3N$ harmonic oscillators)

4.4 Electron-phonon interaction

For simplicity, we only discuss here interaction of electrons with acoustic phonons. Acoustic phonons correspond to a slowly (on the scale of a lattice constant) varying in space displacement of atoms $\mathbf{u}(x)$, which produces the charge $Z\,\mathrm{div}\,\mathbf{u}(x)$ per unit cell (Z is the charge of a single ion). This charge, in turn, results in an electric potential for the electrons. Taking into account screening (see Section 3.3), the electric potential is proportional to this charge, which finally results in the electron-phonon interaction

$$H_{\rm e-ph} = \frac{\rm const}{\nu a_0^3} \int d^3x\, a^+(x) a(x)\ \mathrm{div}\,\mathbf{u}(x)\,, \tag{4.4.1}$$

where ν is the density of states at the Fermi level, a_0 is the lattice constant, and const is some numerical coefficient of order 1. Note that electrons are coupled only to *longitudinal* phonon modes (with the displacements along the k vector).

Next we rewrite the displacement $\mathbf{u}(x)$ in terms of the phonon creation and annihilation operators b_k and b_k^+:

$$\mathbf{u}(x,t) = \int \frac{d^3q}{(2\pi)^3} \frac{a_0^{3/2}}{\sqrt{2M_i\omega_q}} \left(b_q e^{i(qr-\omega_q t)} + b_q^+ e^{-i(qr-\omega_q t)}\right)\,. \tag{4.4.2}$$

where M_i is the mass of an ion and ω_q is the phonon frequency at the wave vector q (derive this formula as a homework). The phonon creation and annihilation operators here are normalized as

$$[b_q, b_{q'}^+] = (2\pi)^3 \delta(q - q')\,. \tag{4.4.3}$$

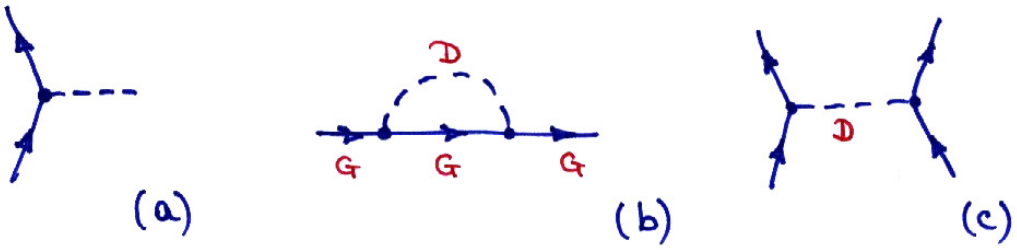

Figure 16: **(a)**: the vertex corresponding to the electron-phonon interaction (4.4.5); **(b)**: The lowest-order diagram describing the renormalization of the electron spectrum due to phonons; **(c)**: The interaction between electrons mediated by phonons.

It turns out to be convenient to define the phonon operator as

$$\varphi(x) = \int \frac{d^3q}{(2\pi)^3} \sqrt{\frac{\omega_q}{2}} \left(b_q e^{iqr} + b_q^+ e^{-iqr} \right) , \tag{4.4.4}$$

which results in the electron-phonon interaction written in the simple form (we used the linear relation $\omega_q = c|q|$):

$$H_{\text{e-ph}} = g \int d^3x \, a^+(x) a(x) \, \varphi(x) \, , \tag{4.4.5}$$

where g is an interaction constant (with the above definitions, $g \sim \nu^{-1/2}$ up to a numerical coefficient)

This electron-phonon interaction can now be incorporated into the diagrammatic approach as a triple vertex (Fig. 16a). One can further derive the Green's function for phonons and construct the perturbative diagrammatic series in the usual way. For example, the leading correction to the electron spectrum due to phonons is given by the diagram in Fig. 16b.

4.5 Green's function for phonons

Similarly to electrons, we define the Green's function for phonons as

$$D(x,t) = -iT\langle \varphi(x,t), \varphi(0,0) \rangle \, . \tag{4.5.1}$$

(T denotes the time ordering). It can be easily computed at zero temperature. Using the definition (4.4.4), and the fact that there are no phonons at zero temperature, we find

$$D(x,t) = -i \int \frac{d^3q}{(2\pi)^3} \frac{\omega_q}{2} \begin{cases} e^{i(qx - \omega_q t)} \, , & t > 0 \, , \\ e^{-i(qx - \omega_q t)} \, , & t < 0 \, . \end{cases} \tag{4.5.2}$$

Performing the Fourier transform in time and space, we find the Green's function of phonons in the frequency-momentum representation:

$$D(q,\omega) = \frac{\omega_q}{2} \left(\frac{1}{\omega - \omega_q + i0} - \frac{1}{\omega + \omega_q - i0} \right) = \frac{\omega_q^2}{\omega^2 - \omega_q^2 + i0} \, . \tag{4.5.3}$$

4.6 Attraction between electrons mediated by phonons

We are now ready to show that interaction with phonons leads to attraction. This attraction appears in the second order of the perturbation theory as the phonon line in the diagram, see Fig. 16c.

For a formal derivation, expand the evolution operator with respect to the electron-phonon interaction:

$$U = e^{-i(H_0+H_{\mathrm{e-ph}})t} = U_0 + U_1 + U_2 + \dots \tag{4.6.1}$$

At the second order of the perturbation theory,

$$U_2 = \iint\limits_{0<t_1<t_2<t} dt_1\, dt_2\, e^{-iH_0(t-t_2)}\,(-iH_{\mathrm{e-ph}})\, e^{-iH_0(t_2-t_1)}\,(-iH_{\mathrm{e-ph}})\, e^{-iH_0 t_1}\,. \tag{4.6.2}$$

If we now substitute the electron-phonon interaction term (4.4.5) and perform the Wick contraction (= averaging) of the phonon operators, we arrive at

$$U_2 = U_0 \iint\limits_{0<t_1<t_2<t} dt_1\, dt_2 \iint d^3x_1\, d^3x_2\, a^+(x_2,t_2)a(x_2,t_2)\, a^+(x_1,t_1)a(x_1,t_1)\times \\ \times\,(-i)g^2 D(x_2-x_1,t_2-t_1)\,. \tag{4.6.3}$$

This equation has the same form as the first-order correction U_1 with the usual density-density interaction, except that this interaction is time dependent. The role of interaction is played by the phonon Green's function $D(x_2-x_1,t_2-t_1)$.

For superconductivity, the interaction averaged over time (or, equivalently, at low frequency) is important. This low-frequency effective interaction is

$$V_{\mathrm{eff}} = D(\omega\to 0) = -g^2\,. \tag{4.6.4}$$

It has a negative sign, which means that it is attractive.

The physical meaning of this interaction is as follows. An electron distorts the crystal lattice (creates a positive charge around itself) which, in turn, attracts other electrons. This interaction is delayed: the characteristic time scale for phonons is ω_D^{-1} while electrons are much faster (their characteristic time scale is ε_F^{-1}). As a result, a moving electron leaves behind itself a positively charged track, which attract other electrons even after the original electron has moved away. This is also a reason why the attraction via phonons is not killed by the Coulomb repulsion of electrons: while the overall magnitudes of these interactions are of the same order, the Coulomb repulsion is instant, and the phonon attraction has a longer time scale and wins at low frequencies. An accurate treatment of this competition of the two interactions is technical and goes beyond the scope of this lecture: see, e.g., the original paper P. Morel and P. W. Anderson, Phys. Rev. **125**, 1263 (1962).

5 BCS theory of superconductivity

Refs: [Mar] Section 27.3, [LP] Sections 39,40.

As we have seen, phonons mediate an attraction between electrons. In this section, we will see how superconductivity emerges in an electron gas with attraction (the theory of Bardeen–Cooper–Schrieffer).

5.1 Superconductivity as spontaneous symmetry breaking

Superconductivity is associated with developing nonzero *anomalous averages*

$$\langle a_\alpha a_\beta \rangle \neq 0 \,, \tag{5.1.1}$$

where a_α and a_β are annihilation operators and α and β denote electron degrees of freedom (momentum/coordinate and spin). Such an average breaks the U(1) (electromagnetic) symmetry

$$a \mapsto e^{i\alpha} a \,, \qquad a^+ \mapsto e^{-i\alpha} a^+ \,. \tag{5.1.2}$$

The anomalous average (5.1.1) may only be nonzero in a superposition of states with different particle numbers. Physically, the number of electrons in an isolated piece of a superconductor is fixed, in which case (5.1.1) should be understood as a long-range order

$$\lim_{|x-y|\to\infty} \langle (a_\alpha a_\beta)_x \, (a^+_\beta a^+_\alpha)_y \rangle \neq 0 \,, \tag{5.1.3}$$

and the phase of an individual average $\langle a_\alpha a_\beta \rangle$ remains undetermined.

A good analogy to think of is the ferromagnetic transition: in a ferromagnet, the average magnetization is non-zero and points in a spontaneously chosen direction, even though in an isolated system, formally, the ground state is a superposition of states with all equivalent orientations of magnetization.

The phase of the average $\langle a_\alpha a_\beta \rangle$ is the spontaneously broken symmetry. It is not observable directly, but only in comparison with other such phases (the *Josephson effect*). A spatial modulation of this phase corresponds to the *supercurrent* (an electric current which propagates without dissipation).

Superconductors may be classified by the symmetry of indices in the anomalous average (5.1.1). The most common symmetry (usually favored in superconductors with attraction due to phonons) is the *s-wave* superconductivity: the spin indices in (5.1.1) form a singlet, and the pairing is isotropic in space.

5.2 Model Hamiltonian and mean-field approximation

We consider a model Hamiltonian of the form

$$H = H_0 + H_{\text{int}} \,, \tag{5.2.1}$$

where

$$H_0 = \sum_{k,\alpha} (\varepsilon_k - \mu) a^+_{k,\alpha} a_{k,\alpha} \tag{5.2.2}$$

is the free part, and

$$H_{\text{int}} = -\frac{1}{2\mathcal{V}} \sum_{\tilde{k}_1, \tilde{k}_2, \tilde{k}_3} a^+_{\tilde{k}_1} a^+_{\tilde{k}_2} a_{\tilde{k}_3} a_{\tilde{k}_1 + \tilde{k}_2 - \tilde{k}_3} V_{\tilde{k}_1, \tilde{k}_2, \tilde{k}_3, \tilde{k}_1 + \tilde{k}_2 - \tilde{k}_3} \,, \tag{5.2.3}$$

where $\mathcal{V}$ is the system volume and $V_{\tilde{k}_1, \tilde{k}_2, \tilde{k}_3, \tilde{k}_4}$ are the interaction matrix elements (the spin indices are included in $\tilde{k}_i$ for simplicity). In this chapter, we use the "sum" notation (the sum over k instead of integration over $d^3k/(2\pi)^3$), with the electronic states normalized as $\{a_k, a^+_{k'}\} = \delta_{kk'}$ (instead of the delta function of the continuous variable $k - k'$).

We will use the *mean-field approximation*: first, replace the products $a_k a_{k'}$ by their nonzero averages and then solve the *self-consistency* equation for those averages.

The structure of the non-zero anomalous averages depends on the interaction $V_{\tilde{k}_1,\tilde{k}_2,\tilde{k}_3,\tilde{k}_4}$. We assume that the superconductor is s-wave, with $\langle a_{k\uparrow} a_{-k\downarrow}\rangle \neq 0$. Correspondingly, we only consider the terms of this type in the interaction and neglect the k dependence of the interaction matrix elements (since, as we will see below, only k values around the Fermi surface are relevant). As a result, we simplify the interaction term to

$$H_{\text{int}} = -\frac{g_0}{\mathcal{V}} \sum_{k,k'} a^+_{k\uparrow} a^+_{-k\downarrow} a_{-k'\downarrow} a_{k'\uparrow} = -\frac{g_0}{\mathcal{V}} \left(\sum_k a^+_{k\uparrow} a^+_{-k\downarrow} \right) \left(\sum_{k'} a_{-k'\downarrow} a_{k'\uparrow} \right) , \tag{5.2.4}$$

where g_0 is some positive interaction constant.

We further define the complex numbers

$$d_k = \langle a_{-k\downarrow} a_{k\uparrow} \rangle \qquad d^*_k = \langle a^+_{k\uparrow} a^+_{-k\downarrow} \rangle . \tag{5.2.5}$$

These numbers will be later determined from the self-consistency conditions.

By replacing the products in the four-fermion operator by their averages, we get the quadratic Hamiltonian

$$H_{\text{BCS}} = \sum_k \left[(\varepsilon_k - \mu)(a^+_{k\uparrow} a_{k\uparrow} + a^+_{-k\downarrow} a_{-k\downarrow}) + \Delta^* a_{-k\downarrow} a_{k\uparrow} + \Delta a^+_{k\uparrow} a^+_{-k\downarrow} \right] , \tag{5.2.6}$$

where

$$\Delta = -\frac{g_0}{\mathcal{V}} \sum_k d_k . \tag{5.2.7}$$

5.3 Bogoliubov quasiparticles and the BCS ground state

This quadratic Hamiltonian may be diagonalized by a rotation in the particle-hole space:

$$\gamma^+_{k\uparrow} = u_k a^+_{k\uparrow} + v_k a_{-k\downarrow} . \tag{5.3.1}$$

The coefficients u_k and v_k can be found, e.g., from the commutation relation

$$[H_{\text{BCS}}, \gamma^+_{k\uparrow}] = \tilde{\varepsilon}_k \gamma^+_{k\uparrow} . \tag{5.3.2}$$

We find the equation on the coefficients:

$$\begin{pmatrix} \varepsilon_k - \mu & \Delta \\ \Delta^* & -(\varepsilon_k - \mu) \end{pmatrix} \begin{pmatrix} u_k \\ v_k \end{pmatrix} = \tilde{\varepsilon}_k \begin{pmatrix} u_k \\ v_k \end{pmatrix} . \tag{5.3.3}$$

The eigenvalues give the spectrum:

$$\tilde{\varepsilon}_k = \pm \sqrt{(\varepsilon_k - \mu)^2 + |\Delta|^2} . \tag{5.3.4}$$

Thus $|\Delta|$ plays the role of the *gap* in the spectrum (see Fig. 17).

The fermionic Fock space may be now represented in terms of the occupation numbers for (Bogoliubov) quasiparticles $\gamma^+_{k\uparrow}$. There are two ways to label quasiparticles:

- We can consider only *spin-up* operators, as in (5.3.2). In this case, we get two solutions for each k vector: one with positive, and one with negative energy.

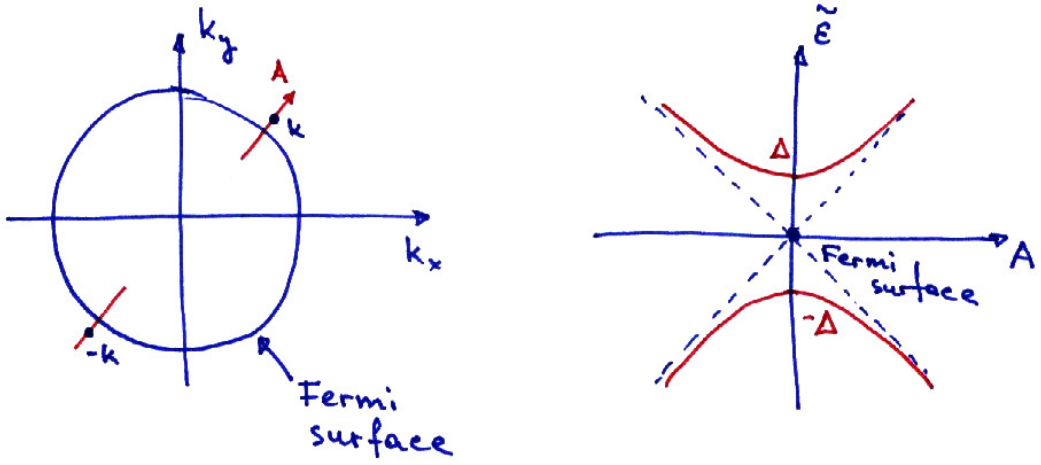

Figure 17: Left: The two sections across the Fermi surface contributing to the spectrum in the right panel. Each quasiparticle in the right panel corresponds to a linear combination of an electron with momentum k and a hole with momentum $-k$ and opposite spin. Right: The BCS spectrum (5.3.4).

- Alternatively, we can re-label the negative-energy solutions (5.3.4) as annihilation operators $\gamma_{-k\downarrow}$. Then, for each k vector, we will have two quasiparticles $\gamma^+_{k\uparrow}$ and $\gamma^+_{k\downarrow}$, both with positive energies.

In any of these notations, the total number of quasiparticle states (the dimension of the Hilbert space) is the same as for original electrons: two single-particle states per k vector. We will use the second notation (with positive-energy quasiparticles).

It will also be convenient to normalize the coefficients so that

$$|u_k|^2 + |v_k|^2 = 1\,. \tag{5.3.5}$$

This would produce the canonical anticommutation relations for the quasiparticles:

$$\{\gamma_{k\alpha}, \gamma^+_{k'\beta}\} = \delta_{kk'}\delta_{\alpha\beta}\,. \tag{5.3.6}$$

The Hamiltonian (5.2.6) can now be written in terms of quasiparticles as

$$H_{\rm BCS} = \sum_k \tilde{\epsilon}_k \left(\gamma^+_{k\uparrow}\gamma_{k\uparrow} + \gamma^+_{k\downarrow}\gamma_{k\downarrow}\right) + E_0\,, \tag{5.3.7}$$

The ground state of the superconductor $|{\rm GS}\rangle$ may be found from the condition that it contains no quasiparticles:

$$\gamma_{k\alpha}|{\rm GS}\rangle = 0\,. \tag{5.3.8}$$

Since sectors with different k vectors are decoupled in the Hamiltonian, this equation can be solved independently for each k vector:

$$|{\rm GS}\rangle_k = (u^*_k - v^*_k a^+_{k\uparrow} a^+_{-k\downarrow})|\star\rangle_k\,, \tag{5.3.9}$$

where $|\star\rangle$ is the state without electrons and the subscript k denotes that only states with a given k vector are considered. Combining all the k vectors together, we find the expression

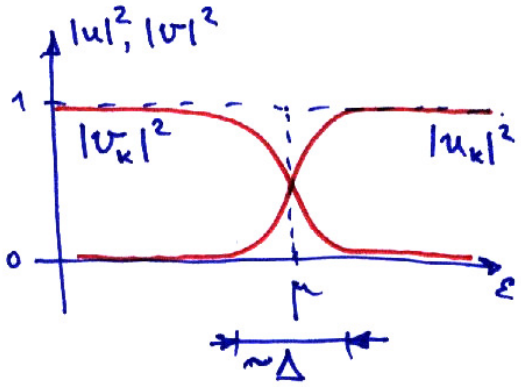

Figure 18: The coherence factors (5.3.11) as a function of energy.

for the ground state of the superconductor:

$$|\mathrm{GS}\rangle = \prod_k (u_k^* - v_k^* a_{k\uparrow}^+ a_{-k\downarrow}^+)|\star\rangle\,. \tag{5.3.10}$$

Note that this state is a superposition of states with different numbers of particles.

If we calculate u_k and v_k explicitly from diagonalizing the matrix (5.3.3), we find

$$\begin{aligned} u_k &= e^{i\varphi}\sqrt{\frac{1}{2}\left(1+\frac{\epsilon_k-\mu}{\tilde{\epsilon}_k}\right)}\,, \\ v_k &= \sqrt{\frac{1}{2}\left(1-\frac{\epsilon_k-\mu}{\tilde{\epsilon}_k}\right)}\,, \end{aligned} \tag{5.3.11}$$

where φ is the phase of Δ. The absolute values of u_k and v_k are plotted in Fig. 18. We see that superconductivity changes the structure of the ground state only in the window of energies of the order Δ around the Fermi level (we usually have $\Delta \ll \mu$ in superconductors).

5.4 Self-consistency equations for the superconducting gap

The anomalous correlation functions d_k and the superconducting gap Δ are determined from the self-consistency conditions (5.2.5), where the averages are calculated in the quadratic system (5.2.6) at a finite temperature T.

One of the possible ways to compute the anomalous average $\langle a_{-k\downarrow} a_{k\uparrow}\rangle$ is to re-express the a operators in terms of the quasiparticles γ and γ^+ and then use the equilibrium Fermi occupation numbers for the quasiparticles:

$$\begin{cases} \gamma_{k\uparrow}^+ = u_k a_{k\uparrow}^+ + v_k a_{-k\downarrow} \\ \gamma_{-k\downarrow} = v_k^* a_{k\uparrow}^+ - u_k^* a_{-k\downarrow} \end{cases} \quad\Rightarrow\quad \begin{cases} a_{k\uparrow}^+ = u_k^* \gamma_{k\uparrow}^+ + v_k \gamma_{-k\downarrow} \\ a_{-k\downarrow} = v_k^* \gamma_{k\uparrow}^+ - u_k \gamma_{-k\downarrow} \end{cases} \tag{5.4.1}$$

In terms of the quasiparticles $\gamma_{k\uparrow}^+$ and $\gamma_{-k\downarrow}$, the BCS Hamiltonian is diagonal, so we find

$$\langle a_{-k\downarrow} a_{k\uparrow}\rangle_T = v_k^* u_k \langle \gamma_{k\uparrow}^+ \gamma_{k\uparrow} - \gamma_{-k\downarrow}\gamma_{-k\downarrow}^+\rangle_T = v_k^* u_k\,[2n_F(\tilde{\varepsilon}_k) - 1] = -v_k^* u_k \tanh\frac{\tilde{\varepsilon}_k}{2T}\,, \tag{5.4.2}$$

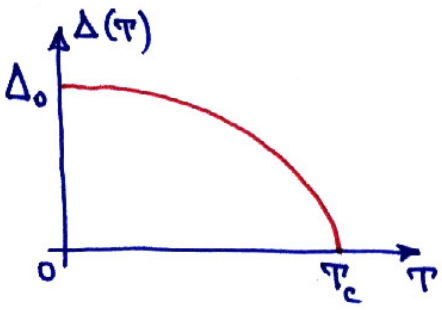

Figure 19: A sketch of the gap dependence on the temperature.

where $\tilde{\varepsilon}_k$ is the quasiparticle energy given by Eq. (5.3.4).

Substituting this into Eq. (5.2.7), we find the self-consistency equation for the gap

$$\Delta = \frac{g_0}{\mathcal{V}} \sum_k v_k^* u_k \tanh \frac{\tilde{\varepsilon}_k}{2T} \,. \tag{5.4.3}$$

Using Eq. (5.3.11) for u_k and v_k, we find

$$v_k^* u_k = \frac{\Delta}{2\tilde{\varepsilon}_k} \,. \tag{5.4.4}$$

Note that this quantity is significant only in the vicinity of the Fermi surface (since far away form the Fermi surface either u_k or v_k tends to zero).

We remark that $\Delta = 0$ is always a formal solution to the equations (5.4.3)–(5.4.4). But one can show that at low temperatures this solution does not correspond to a minimum of a free energy, but to its maximum. In other words, at low temperatures the $\Delta = 0$ solution is unstable, and the physically relevant solution is a nontrivial one. To find this nontrivial solution, we divide the equation by Δ and replace the sum over k by integration over energies:

$$\frac{1}{\mathcal{V}} \sum_k \quad \to \quad \nu_0 \int d\varepsilon \,, \tag{5.4.5}$$

where ν_0 is the density of electronic states (for free electrons) per unit volume and per spin projection and ε is the free-electron energy. Substituting equation (5.3.4) for $\tilde{\varepsilon}_k$ and shifting the integration variable to $\varepsilon = \varepsilon_k - \mu$, we finally find the self-consistency equation in the closed form

$$1 = g_0 \nu_0 \int d\varepsilon \frac{\tanh \frac{\sqrt{\varepsilon^2 + |\Delta|^2}}{2T}}{2\sqrt{\varepsilon^2 + |\Delta|^2}} \,. \tag{5.4.6}$$

This equation, in principle allows to determine Δ as a function of temperature (see Fig. 19).

5.5 Superconducting gap at zero temperature

A subtle point in this calculation is that the integral (5.4.6) actually diverges logarithmically at large ε. Physically, this divergence is removed by introducing a cut-off at energies

of the order of Debye energy ω_D (since the attraction mediated by phonons only extends to those energies).

At zero temperature, $\tanh(\ldots) \to 1$, and the equation (5.4.6) reduces to

$$1 = g_0\nu_0 \int_0^{\sim\omega_D} \frac{d\varepsilon}{\sqrt{\varepsilon^2+\Delta_0^2}} = g_0\nu_0 \left[\ln\frac{\omega_D}{\Delta_0} + \text{const}\right], \tag{5.5.1}$$

where const is a constant of order one. This gives the superconducting gap at zero temperature Δ_0 in the form

$$\Delta_0 = \text{const}\ \omega_D \exp\left(-\frac{1}{g_0\nu_0}\right). \tag{5.5.2}$$

Note that the gap is exponentially small in g_0.

5.6 Superconducting transition temperature

In a similar way we can find the superconducting transition temperature T_c, with the only difference that now we neglect Δ in the self-consistency equation (5.4.6):

$$1 = g_0\nu_0 \int_0^{\sim\omega_D} d\varepsilon \frac{\tanh\frac{\varepsilon}{2T_c}}{\varepsilon} = g_0\nu_0 \left[\ln\frac{\omega_D}{T_c} + \text{const}\right], \tag{5.6.1}$$

with some const of order one (but different from that in the calculation of Δ_0 above!). In other words, T_c is of the same order of magnitude as Δ_0.

Remarkably, one can determine the ratio T_c/Δ_0 without any ambiguity related to the cutoff. Namely, the difference of the integrals (5.5.1) and (5.6.1) is convergent and does not depend on the cut-off:

$$0 = \int_0^\infty d\varepsilon \left[\frac{\tanh\frac{\varepsilon}{2T_c}}{\varepsilon} - \frac{1}{\sqrt{\varepsilon^2+\Delta_0^2}}\right] = \int_0^\infty dx \left[\frac{\tanh(x/2)}{x} - \frac{1}{\sqrt{x^2+(\Delta_0/T_c)^2}}\right]. \tag{5.6.2}$$

From this equation, one finds the *universal* value for the ratio T_c/Δ_0:

$$T_c \approx 0.57\Delta_0\,. \tag{5.6.3}$$

[This value is easy to obtain by numerical methods. A more sophisticated analytic calculation gives

$$T_c = \left(\frac{e^C}{\pi}\right)\Delta_0\,, \tag{5.6.4}$$

where $C = 0.577\ldots$ is the Euler constant].

The relation (5.6.3) is in a remarkably good agreement with experimental values on many conventional superconductors, despite the simplifications made in the BCS theory.

6 Problem Sets

6.1 Problem Set 1

Problem 1.1.

(a) Complete the derivation (1.2.6). Verify that for the Sommerfeld model (free fermions), the result reduces to the expression (1.1.8).

(b) For copper, compare the experimentally measured electronic specific heat with the free-fermion expression (1.1.8). Experimental data are available, e.g., in the papers

- D. W. Osborne, H. E. Flotow, and F. Schreiner, Rev. Sci. Instrum. **38**, 159 (1967).
- M. Hurley and B. C. Gerstein, J. Chem. Thermodynamics **6**, 787 (1974).

(remember that you need the low-temperature limit for comparison)

Problem 1.2

(a) Show that both expressions (1.2.10) and (1.2.12) are proportional to the integral over the Fermi surface

$$\int dS \frac{v_\alpha v_\beta}{v} \,. \tag{6.1.1}$$

(b) Calculate the coefficients and demonstrate the Wiedemann–Franz law (1.1.9).

(c) In the model of free fermions (Sommerfeld theory), show that the results for σ and κ reduce to Eqs. (1.1.2) and (1.1.3), respectively.

(d) Find in the literature the electrical conductivity of copper at room temperature. Within the free-fermion theory, estimate (by the order of magnitude) the relaxation time τ and the mean free path $l = \tau v_F$. How does it compare with the lattice constant? Is the quasiclassical approximation justified?

6.2 Problem Set 2

Problem 2.1

(a) Construct the character table for the group D_4 of all the symmetries of a square, including rotations and reflections. How many irreducible representations are there? Can you also construct those representations explicitly?

(b) Consider a single quantum particle hopping between the four corners of a square. The hopping amplitude along each side of the square is $-t_1$ and along each of the two diagonals $-t_2$. The Hamiltonian of the particle can be written as the matrix

$$H = \begin{pmatrix} 0 & -t_1 & -t_2 & -t_1 \\ -t_1 & 0 & -t_1 & -t_2 \\ -t_2 & -t_1 & 0 & -t_1 \\ -t_1 & -t_2 & -t_1 & 0 \end{pmatrix} . \tag{6.2.1}$$

Find the spectrum of this Hamiltonian and classify the levels according to the representations of D_4.

(c) Suppose now that the square is stretched along the axis parallel to a pair of sides (so that the hopping coefficients t_1' along this direction and t_1'' along the perpendicular direction become different). How will the energy levels split?

(d) The same question if the square is stretched along one of the diagonals (so that the two coefficients along the two diagonals t_2' and t_2'' become different).

6.3 Problem Set 3

Problem 3.1

In the numerical calculation, the valence band at point Γ is three-fold degenerate and belongs to the representation Γ_{25}'. How does this three-fold degeneracy split along the lines $\Gamma - X$ and $\Gamma - L$? Calculate the result by treating Γ_{25}' as a representation of the small point group and by decomposing it into irreducible representations.

Problem 3.2

If one adds a potential to the free-electron band structure in Fig. 3, how would the 8-point degenerate level at the Γ point split? Hint: this degenerate level comes from the eight nearest-neighbor k points of the dual lattice in Fig. 2. They transform into each other under the O_h group as eight vertices of the cube.

6.4 Problem Set 4

Problem 4.1

(a) Verify the following identities for commutators $[A, B] = AB - BA$ and anticommutators $\{A, B\} = AB + BA$:

$$[A, BC] = [A, B]\, C + B\, [A, C] = \{A, B\}\, C - B\, \{A, C\} \tag{6.4.1}$$

$$\{A, BC\} = [A, B]\, C + B\, \{A, C\} = \{A, B\}\, C - B\, [A, C] \tag{6.4.2}$$

These relations [called the distributive law for commutators] are helpful for commuting products of creation and annihilation operators.

Note: always use commutators for bosonic operators and anticommutators for fermionic operators. Products of an even number of fermionic operators count as bosonic operators.

(b) Verify by an explicit calculation that the free-particle Hamiltonian

$$H = \int \frac{d^3k}{(2\pi)^3}\, a_k^+ (\varepsilon_k - \mu) a_k\,, \tag{6.4.3}$$

commutes with the particle-number operator

$$N = \int \frac{d^3k}{(2\pi)^3}\, a_k^+ a_k\,, \tag{6.4.4}$$

Hint: the calculation can be simplified by using the relations derived in part (a).

Problem 4.2

Consider one fermionic level. The Fock space consists of two states: empty $|0\rangle$ (0 particles) and occupied $|1\rangle$ (1 particle). The fermionic creation and annihilation operators act as

$$a\,|0\rangle = 0\,, \qquad a\,|1\rangle = |0\rangle\,, \tag{6.4.5}$$

$$a^+\,|0\rangle = |1\rangle\,, \qquad a^+\,|1\rangle = 0\,. \tag{6.4.6}$$

(a) Verify the anticommutation relations

$$\{a, a^+\} = 1\,, \qquad \{a, a\} = \{a^+, a^+\} = 0\,. \tag{6.4.7}$$

(b) Now suppose that the particle has a positive energy, and therefore at zero temperature the system is in the ground state $|0\rangle$. Verify that, in this state, the Wick theorem (3.1.34) holds for the product of four operators aa^+aa^+:

$$\langle aa^+aa^+\rangle_{T=0} = \ldots \tag{6.4.8}$$

(c) At a finite temperature, the system will be at a statistical mixture of two states: the state $|0\rangle$ with a probability p and the state $|1\rangle$ with the probability $1-p$. Verify that the Wick theorem for the expectation value $\langle aa^+aa^+\rangle$ still holds.

6.5 Problem Set 5

Problem 5.1

(a) In the subsection 3.1.7, we neglected the spin of the electrons. How would the results change, if we include spin?

(b) Consider the model of free electrons with Coulomb interaction. Assume the free-particle kinetic energy $\varepsilon_k = \hbar^2 k^2/(2m)$ and calculate, at zero temperature, the average interaction energy per particle, using the perturbative expression (3.1.43). Do not forget about spin! Express your result as

$$\delta E = \varepsilon_F\, f\left(\frac{r_s}{a_0}\right)\,, \tag{6.5.1}$$

where ε_F is the Fermi energy and r_s/a_0 is the dimensionless parameter introduced in Section 1.1.5:

$$r_s = \left(\frac{3}{4\pi n}\right)^{1/3}\,, \qquad a_0 = \frac{\hbar^2}{me^2} = 0.529\text{Å} \tag{6.5.2}$$

(a typical distance between electrons in the units of the Bohr radius). Find the function f. If you encounter difficulties in computing integrals, you may either compute them numerically (using your favorite software) or leave them uncomputed as unknown *numerical* coefficients.

Note that we only consider the correction (3.1.43), but not (3.1.42), since the latter is exactly canceled by the background positive charge of the ions.

(c) From the result of part (b), show the stability of a metal: minimize the total energy per electron

$$E_{\text{tot}} = E_{\text{kin}} + \delta E \tag{6.5.3}$$

as a function of r_s. The average kinetic energy per particle E_{kin} is proportional to ε_F. Remember that ε_F itself depends on r_s:

$$\varepsilon_F = \frac{\hbar^2 k_F^2}{2m} = \left(\frac{9\pi}{4}\right)^{2/3} \left(\frac{a_0}{r_s}\right)^2 \text{Ry}\,, \qquad \text{Ry} = \frac{\hbar^2}{2ma_0^2} \approx 13.6\,\text{eV} \tag{6.5.4}$$

If you have calculated the numerical coefficient in part (b), use it to find the optimal value of r_s. Compare it to the actual values of r_s in alkali metals (Li, Na, K: they are the closest to the free-fermion model).

(d)* In the model of free electrons with Coulomb interaction [the same as in parts (b) and (c)], calculate the correction to the energy of a particle at a wave vector k close to the Fermi surface, as given by Eq. (3.1.44). You should find a logarithmic divergence of the Fermi velocity. Show that this divergence comes from the long-range part of the Coulomb potential (since our calculation does not include screening).

6.6 Problem Set 6

Problem 6.1

(a) For a free particle in 3D, calculate the Green's functions $G_\omega(R)$ [in the frequency-coordinate representation, as defined in Eq. (3.2.4)]. In order to do this, calculate the three-dimensional version of the integral (3.2.18).

As in 2D, this Green's functions oscillates at the wave vector $k_\omega = \sqrt{2m\omega}$ and decays as a power of R. Compare this power with $R^{-1/2}$ for the 2D Green's function (3.2.22).

(b) If we study the effect discussed in Section 3.2.2 (density-of-states oscillations around an impurity) in 3D, then, at large R we would find

$$\delta\rho_\omega(R) \propto R^{-\alpha} \cos(2k_\omega R + \varphi)\,. \tag{6.6.1}$$

Find the power α.

6.7 Problem Set 7

Problem 7.1 Time-ordered Green's function.

(a) Using the results of Problem 6.1 for the single-particle Green's function, find the *time-ordered* Green's function $G^c_\omega(R)$ of a free Fermi gas in 3D. You may use the relations (3.2.30) and (3.2.31).

(b) By an explicit integration of $G^c_\omega(R)$, check that

$$G^c(t{=}0, R) = \int_{-\infty}^{+\infty} \frac{d\omega}{2\pi}\, G^c_\omega(R) \tag{6.7.1}$$

coincides with the Green's function (3.1.38).

Problem 7.2 RKKY interaction.

(a) RKKY (Ruderman–Kittel–Kasuya–Yosida) interaction is a mechanism of coupling of localized magnetic moments (nuclear magnetic moments or spins of localized electrons in inner shells) through conduction electrons. The physics of mechanism is as follows: If we have a localized magnetic moment $\mathbf{S}$, it couples locally to electrons via

$$H_{\text{int}} = \alpha\, \mathbf{S}\, a^+_\alpha(x)\, \sigma_{\alpha\beta}\, a_\beta(x)\,. \tag{6.7.2}$$

Without loss of generality, assume that $\mathbf{S} \parallel \mathbf{z}$. Then it is equivalent to the potential $\pm\alpha S$ at the position x for up/down spins respectively. This potential leads to the modulation of density (the actual density, not the density of states!)

$$\delta n_\uparrow(y) = U(x-y)\,\alpha S\,, \qquad \delta n_\downarrow(y) = -U(x-y)\,\alpha S \tag{6.7.3}$$

with some function $U(x-y)$. If there is another local spin at the position y, this modulation of electronic density leads to the interaction between the two magnetic moments given by

$$E_{\text{RKKY}} = 2\alpha^2\, \mathbf{S}_1\mathbf{S}_2\, U(x-y)\,. \tag{6.7.4}$$

Our goal is to calculate the function $U(x-y)$. It is a linear response of the density δn at the position y to the potential at the position x. Show that this response function is given by the same diagram in Fig. 9, with the only difference that now we integrate over the time difference at the positions x and y and use the time-ordered Green's function. In the frequency representation, it is given by

$$U(R) = \int \frac{d\omega}{2\pi}\, [G^c_\omega(R)]^2 \tag{6.7.5}$$

(where, as usual, we denote $R = |x-y|$). Use what you know from Problems 6.1 and 7.1 to compute this function. You should get

$$U(R) = \frac{1}{16\pi^3}\,\frac{m}{R^4}\,\left[2k_F R\cos(2k_F R) - \sin(2k_F R)\right]\,. \tag{6.7.6}$$

If you are interested, you can take a look at the original paper M. A. Rudermann and C. Kittel, Phys. Rev. **96**, 99 (1954).

(b) In the experimental paper S. S. P. Parkin and D. Mauri Phys. Rev. B **44**, 7131 (1991), the authors observe RKKY-type oscillations in magnetic coupling of two $Ni_{80}Co_{20}$ layers through a thin layer of Ruthenium. They compare their results to the theoretical prediction $U(R) \propto R^{-p}\sin(2k_F R + \phi)$ with $p = 2$. Explain this power dependence on R.

6.8 Problem Set 8

Problem 8.1

Estimate the screening length in a typical metal.

Problem 8.2

Starting from Eq. (3.3.12), derive the results (3.3.13)–(3.3.14) and (3.3.15).

Hint: in calculating the integrals leading to (3.3.14), first integrate over the angular coordinates. When integrating over R, it may be helpful to integrate by parts to reduce the power of R in the denominator and use the following formula:

$$\int_{\epsilon}^{\infty} \frac{e^{ikx}}{x}\, dx = C_0 - \ln(\epsilon|k|) + o(\epsilon)\,, \tag{6.8.1}$$

where C_0 is some constant (which will drop out from the result) and ϵ is a small cut-off (which will be set to zero at the end of the calculation).

6.9 Problem Set 9

Problem 9.1

Compare the specific heat of phonons and electrons in a typical metal [as an example, think of potassium (K) with $\omega_D \sim 100$K and $\varepsilon_F \sim 2 \cdot 10^4$K]:

(a) Consider first the high-temperature limit, $T \geq \omega_D$ (but still $T \ll \varepsilon_F$). In this limit, the phonon contribution is $c_{\text{phonon}} \approx 3N$. Assuming that there is one conduction electron per atom, estimate the relative contribution of electrons to the specific heat.

Hint: you should obtain the result $c_{\text{elec}}/c_{phonon} \sim (T/\varepsilon_F) \ll 1$.

(b) Consider now the limit of low temperatures, $T \ll \omega_D$, where the phonon specific heat is proportional to T^3. Estimate the temperature T^*, below which the electron specific heat dominates over that of phonons.

Hint: you should find $T^* \sim \omega_D^{3/2} \varepsilon_F^{-1/2} \ll \omega_D$.

Problem 9.2

(a) Derive the coefficient in (4.4.1) up to a numerical coefficient of order one.

(b) Consider a one-dimensional model of a solid: a chain of points of mass M_i connected with springs of stiffness K (see Fig. below). The Hamiltonian reads

$$H = \sum_i \frac{p_i^2}{2M_i} + \sum_i K \frac{(x_i - x_{i+1})^2}{2}\,. \tag{6.9.1}$$

Treat this Hamiltonian as quantum-mechanical, find the spectrum and represent the vibrations as bosonic operators b_q and b_q^+. Normalize these operators as in (4.4.3) and derive Eq. (4.4.2) for the displacement x_i.

(c) With the phonon operator defined as in (4.4.4), derive the coefficient g in (4.4.5) up to a numerical coefficient of order one and show that $g \sim \nu^{-1/2}$.

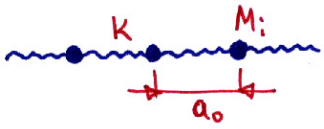

Figure 20: A one-dimensional model of a crystal lattice.

6.10 Problem Set 10

Problem 10.1

By diagonalizing the matrix in (5.3.3), derive the spectrum (5.3.4) and the eigenvectors (5.3.11).

Problem 10.2

(a) In superconductors, there is a characteristic length scale ξ called the *coherence length*. One of its possible definitions is the extent of the pair correlations. Consider the anomalous correlations in real space

$$\Delta(x-y) = \langle a_\downarrow(x) a_\uparrow(y) \rangle \tag{6.10.1}$$

It decays at a certain length scale ξ. Calculate this length in the BCS ground state.

Hint 1: In the BCS ground state, different wave vectors k are decoupled, so it is convenient to do a calculation at a given k vector, and then Fourier transform.

Hint 2: Only a vicinity of the Fermi surface contributes to this anomalous correlator, so you may linearize the electron spectrum near the Fermi surface.

Hint 3: You will find $\xi = v_F/\Delta$.

(b) For Aluminum, find in the literature the value of the gap Δ and estimate the superconducting coherence length ξ.